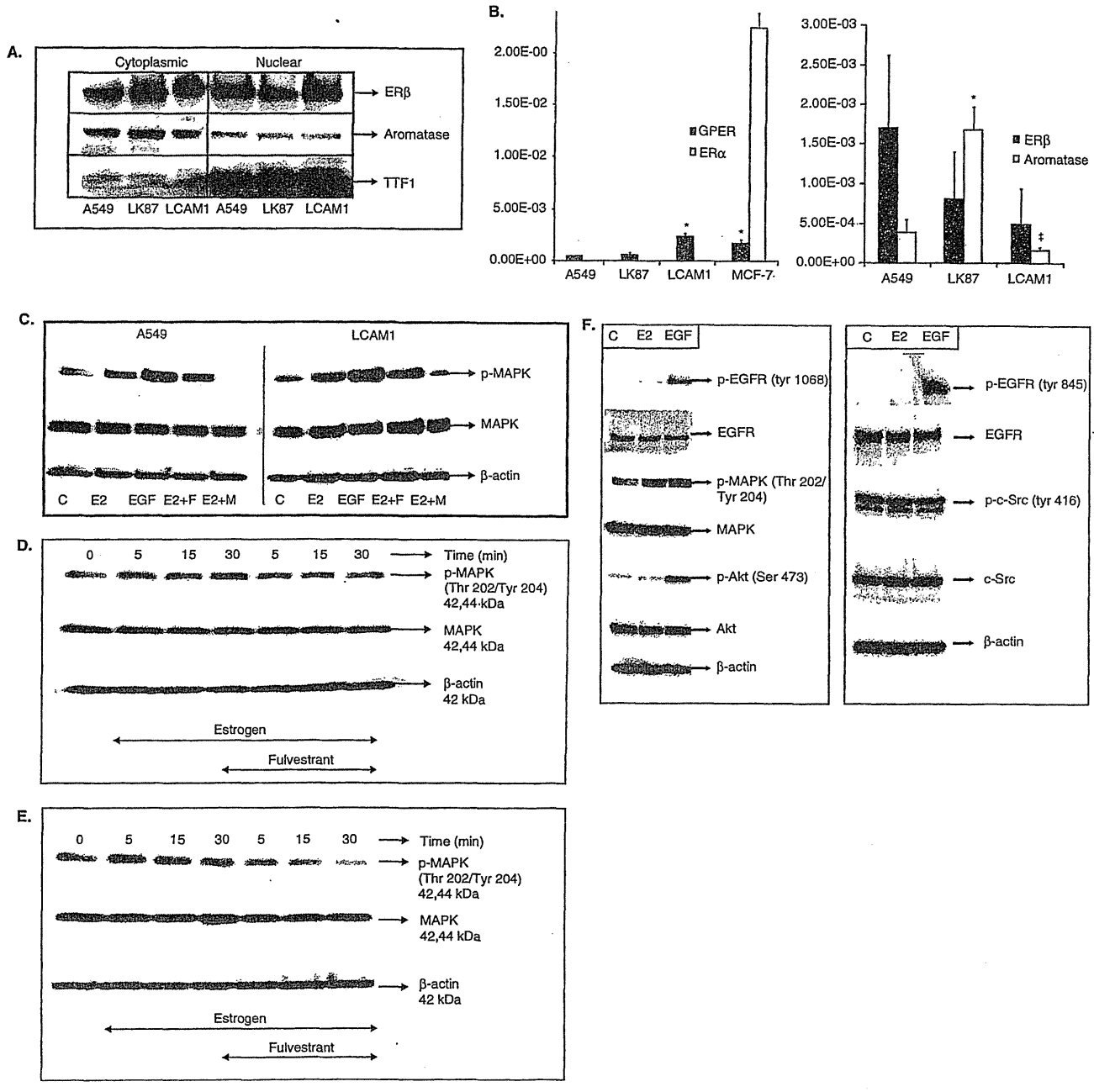

Figure 2. All immunoblots are representative of three independent experiments. A. Expression and localization of ERβ and aromatase in NSCLC cell lines. **B.** Expression of ERα, GPER, ERβ and aromatase in NSCLC cells. **C.** MAPK activation in A549 and LCAM1 cells within 5 min of either estrogen (E2) or EGF treatment and its abrogation by U0126. Abrogation of the MAPK activation caused by E2 treatment on pretreatment with ER blocker, ICI 182780 for 24 h Letrozole (Letro). in **D.** A549 cells and **E.** LCAM1 cells. **F.** Activation of various protein kinases within 5 min of treatment with either E2 or EGF in A549 cells.

F: ER blocker Fulvestrant; M: MAPK inhibitor U0126.

*represents $p < 0.0001$ vs. control.

†represents $p < 0.0001$ vs. either testosterone treatment or E2 and/or EGF treatments.

female nonsmokers was also confined to these elderly women [31]. However, among NSCLC patients, intratumoral concentration of estradiol was significantly higher in men than postmenopausal women [17] and males frequently co-express ERs and aromatase [18]. Therefore, ER pathway is postulated to be also active in males with NSCLC, although it awaits further investigations for clarification of its significance. In addition, among all the patients examined,

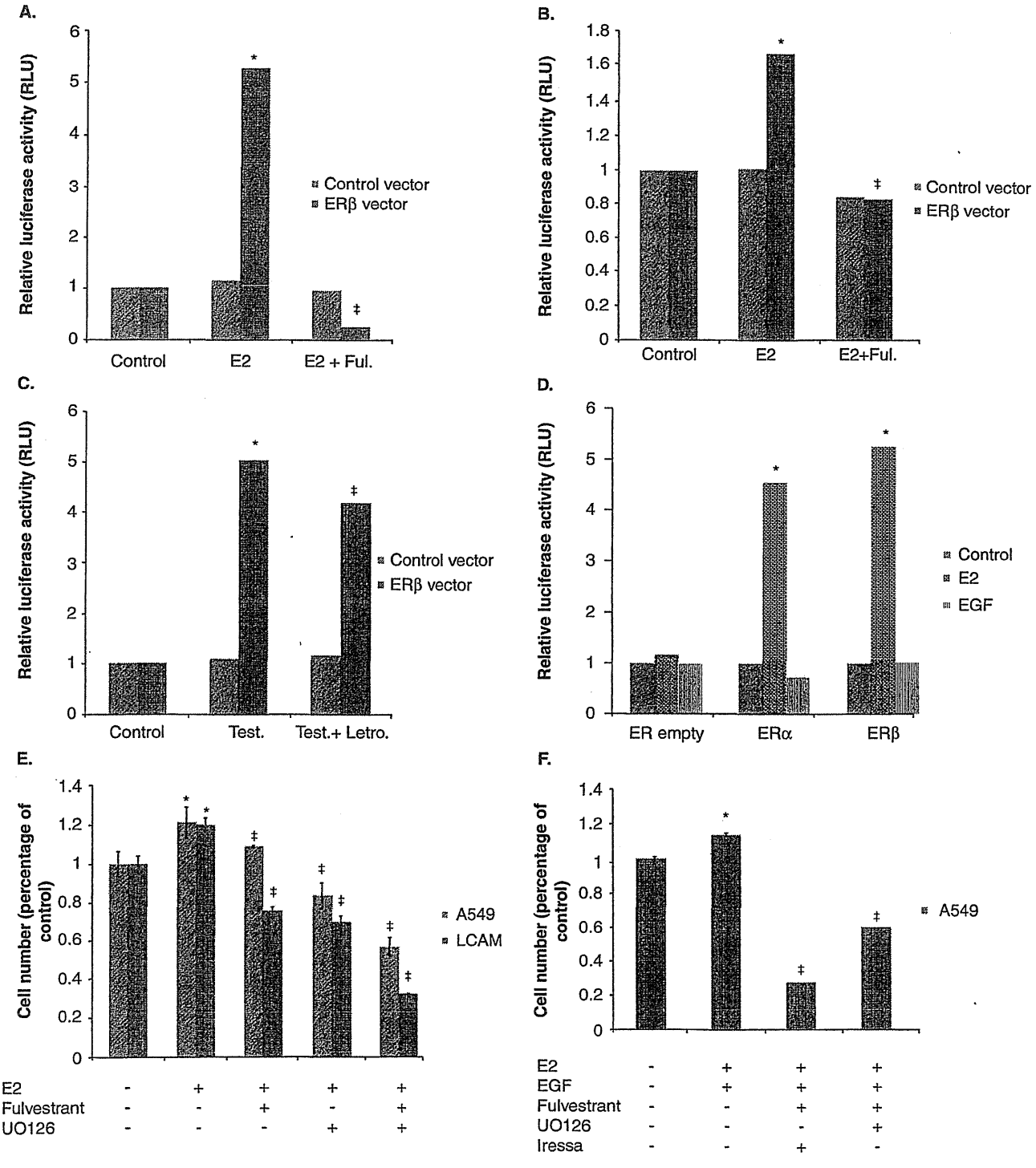

Figure 3. ERE-Luciferase activity (relative light units (RLU)) on treatment with E2 A. A549 cells. **B.** LCAM1 cells (Ful: fuvestrant). **C.** ERE-Luciferase activity on treatment with testosterone in A549 cells. **D.** ERE-luciferase activity in ER empty, ERα and ERβ vector transfected A549 cell on treatment with either estrogen or EGF. **E.** Proliferative effects after 72 h of treatment in A549 and LCAM1 cells. **F.** Anti-proliferative effects of combination therapy with Iressa and fulvestrant versus combination therapy with U0126 and fulvestrant after 48 h of treatment in A549 cells. Data represent three independent experiments, each performed in triplicate. Results are represented as mean ± SD.

*Represents $p < 0.0001$ vs. control.

†Represents $p < 0.0001$ vs. either testosterone treatment or E2 and/or EGF treatments.

the presence of c-ERβ was associated with poorer 5 year survival and median survival rates (c-ERβ positive = 54.8% and 1992 days versus c-ERβ negative = 62.0% and 2805 days, respectively), although the correlation did not reach statistical significance (Figure 1D, Table 4). A similar non-significant tendency was detected when ERβ expression was demonstrated either as a continuous variable or as a dichotomized variable (high versus low). These findings suggest that neither c-ERα, nor n-ERβ 1s a predictor of survival in NSCLC patients [32]. However, c-ERβ was very recently demonstrated to be an important predictor of poorer survival in both men and women with lung cancer [30]. Results of our study also suggested that there were subgroups in which c-ERβ may enhance the estrogenic signaling in NSCLC patients in addition to the genomic actions via n-ERβ. However, the relatively small sample size examined in our present study limited our ability to clearly detect significant prognostic effects of c-ERβ in these patients. Therefore, further studies such as an examination of a large patient cohort are definitely required to obtain better understanding of the potential roles of c-ERβ as predictive biomarker NSCLC patients.

Endogenous levels of c-ERβ and/or n-ERβ could not bring any genomic activity via ERE segments on DNA in the presence of either exogenous E2 or endogenous E2 produced via aromatase activity in A549 and LCAM1 cells, (Figure 3A - C). This may be due to insufficient n-ERβ expression level [12] and/or inability of c-ERβ to translocate into the nucleus after ligand binding [14]. In addition, both ERβ- and ERα-transfected A549 cells demonstrated much higher luciferase activity following E2 treatment but not on EGF treatment, (Figure 3D) which also ruled out any ligand-independent activation of ERs and once again suggested more pronounced roles of ERβ in NSCLC cells. However, ERs can regulate gene expression via non-ERE segments by interacting with the DNA-bound transcription factors [33,34]. Therefore, further investigations are required for better clarification of genomic effects on estrogen in NSCLCs.

In breast carcinoma cells, ERs transactivate membrane EGFR via non-receptor kinases, such as c-Src to rapidly signal through various kinase cascades [16]. Similar transactivation of the EGFR via ERs on ligand binding was reported in 201T cells, a NSCLC cell line [6] even though other investigators did not demonstrate a similar transactivation of EGFR in NSCLC cells [12,14]. We detected only MAPK activation on E2 treatment within 5 min with no transactivation of either EGFR or Akt or c-Src in A549 cells, which was successfully abrogated by 30 min pretreatment with an MAPK inhibitor, (Figure 2C). In addition, pretreatment of NSCLC cells with ER blocker, fulvestrant, for 24 h successfully abrogated this MAPK activation in either A549 and LCAM1 cells, (Figure 1D and E). The fact that a pure ER antagonist, fulvestrant, cannot behave as an antagonist for GPER suggest that estrogen triggered MAPK activation was in fact caused via c-ERβ after ligand binding and not via GPER [35]. Previous reported studies did not necessarily use any ER blocker(s) to confirm whether MAPK or Akt activation on E2 treatment involves mainly membrane/cytoplasmic pools of ERs or GPER. Results of our present study also suggest that c-ERβ on ligand binding may transactivate MAPK without any transactivation of EGFR, (Figure 2F) and MAPK inhibitor could be used very effectively for abrogation of these non-genomic actions of estrogen in NSCLCs.

In addition, the combination therapy with U0126 resulted in enhanced synergistic and additive anti-proliferative effects in A549 and LCAM1 cells respectively than either treatment alone, (Figure 3E). Furthermore, fulvestarnt alone was able to abrogate proliferative effects of estrogen suggesting the possible presence of genomic estrogen signaling via non-ERE segments. However, it is also true that the EGFR pathway was reported to be activated when estrogen was depleted in NSCLC cells and thus simultaneous therapies targeting both pathways are reasonably considered most beneficial in the patients with NSCLC [6]. It was recently demonstrated that estrogen downregulates EGFR levels and tamoxifen upregulates EGFR level in NSCLC cells [36]. These results all suggested that at any given time either the E2 pathway or EGFR is activated in NSCLC cells. In addition, a high c-ERβ along with a high EGFR and low progesterone receptor status in NSCLC patients were reported to predict poorer survival suggesting a close association between ER and EGFR [30]. Therefore, systematic examination of c-ERβ along with EGFR in NSCLC patients could ultimately identify the patients who may benefit most from anti-hormonal therapy, anti-EGFR therapy or combination of both but further investigations are required for clarification. However NSCLC patients invariably develop resistance to EGFR tyrosine kinase inhibitors and the MAPK inhibitor, U0126, has been used by investigators in order to overcome this resistance, in NSCLC cells [37]. Therefore, the combination therapy with both U0126 and fulvestrant may also confer therapeutic benefits to ER expressing NSCLC patients who develop resistance to EGFR-TKI, such as Iressa.

5. Conclusion

The results of our present study suggest that c-ERβ and n-ERβ may result in more aggressive tumor progression in NSCLC patients expressing aromatase. Therefore, targeting both genomic or/and non-genomic estrogen signaling may confer therapeutic benefits to patients expressing both c-ERβ and n-ERβ. However, these findings are also limited by unavailability of a standardized IHC assay for the measurement of ERs in lung cancer and the relatively small number of specimens available for our present study. Therefore, a standard IHC method must be explored in order to understand the clinical significance of ERs in a large cohort of NSCLC patients.

Acknowledgements

We thank the Biomedical Research Core of Tohoku University Graduate School of Medicine for technical support.

Declaration of interest

Y Miki and H Sasano received research funding from CHUGAI pharmaceutical company, Japan. The remaining authors declare no conflict of interest.

Bibliography

1. Parkin DM, Bray F, Ferlay J, Pisani P. Global cancer statistics, 2002. CA Cancer J Clin 2005;55:74-108
2. Siegfried JM. Women and lung cancer: does oestrogen play a role? Lancet Oncol 2001;2:506-13
3. Canver CC, Memoli VA, Vanderveer PL, et al. Sex hormone receptors in non-small-cell lung cancer in human beings. J Thorac Cardiovasc Surg 1994;108:153-7
4. Omoto Y, Kobayashi Y, Nishida K, et al. Expression, function, and clinical implications of the estrogen receptor beta in human lung cancers. Biochem Biophys Res Commun 2001;285:340-7
5. Schwartz G, Prysak GM, Murphy V, et al. Nuclear estrogen receptor beta in lung cancer: expression and survival differences by sex. Clin Cancer Res 2005;11:7280-7
6. Stabile LP, Lyker JS, Gubish CT, et al. Combined targeting of the estrogen receptor and the epidermal growth factor receptor in non-small cell lung cancer shows enhanced antiproliferative effects. Cancer Res 2005;65:1459-70
7. Marquez-Garban DC, Chen HW, Fishbein MC, et al. Estrogen receptor signalling pathways in human non-small cell lung cancer. Steroids 2007;72:135-43
8. Bardin A, Boulle N, Lazennec G, et al. Loss of ERbeta expression as a common step in estrogen-dependent tumor progression. Endocr Relat Cancer 2004;11:537-51
9. Skliris GP, Leygue E, Watson PH, Murphy LC. Estrogen receptor alpha negative breast cancer patients: estrogen receptor beta as a therapeutic target. J Steroid Biochem Mol Biol 2008;109:1-10
10. Matsuyama S, Ohkura Y, Eguchi H, et al. Estrogen receptor beta is expressed in human stomach adenocarcinoma. J Cancer Res Clin Oncol 2002;128:319-24
11. Matthews J, Gustafsson JA. Estrogen signaling: a subtle balance between ERalpha and ERbeta. Mol Interv 2003;3:281-92
12. Hershberger PA, Stabile LP, Kanterewicz B, et al. Estrogen receptor beta (ERbeta) subtype-specific ligands increase transcription, p44/p42 mitogen activated protein kinase (MAPK) activation and growth in human non-small cell lung cancer cells. J Steroid Biochem Mol Biol 2009;116:102-9
13. Hershberger PA, Vasquez AC, Kanterewicz B, et al. Regulation of endogenous gene expression in human non-small cell lung cancer cells by estrogen receptor ligands. Cancer Res 2005;65:1598-605
14. Zhang GF, Liu X, Farkas AM, et al. Estrogen receptor beta functions through nongenomic mechanisms in lung cancer cells. Mol Endocrinol 2009;23:146-56; Erratum in Mol Endocrinol 2010;24:471
15. Pietras RJ, Marquez DC, Chen HW, et al. Estrogen and growth factor receptor interactions in human breast and non-small cell lung cancer cells. Steroids 2005;70:372-81
16. Levin ER. Bidirectional signaling between the estrogen receptor and the epidermal growth factor receptor. Mol Endocrinol 2003;17:309-17
17. Niikawa H, Suzuki T, Suzuki S, et al. Intratumoral estrogens and estrogen receptors in non-small cell lung carcinoma. Clin Cancer Res 2008;14:4417-26
18. Abe K, Miki Y, Sugawara S, et al. Highly concordant coexpression of aromatase and estrogen receptor beta in non-small cell lung cancer. Hum Pathol 2010;41:190-8
19. Oyama T, Kagawa N, Sugio K, et al. Expression of aromatase CYP19 and its relationship with parameters in NSCLC. Front Biosci 2009;14:2285-92
20. Mah V, Seligson DB, Li A, et al. Aromatase expression predicts survival in women with early-stage non-small cell lung cancer. Cancer Res 2007;67:10484-90
21. Weinberg OK, Marquez-Garban DC, Fishbein MC, et al. Aromatase inhibitors in human lung cancer therapy. Cancer Res 2005;65:11287-91
22. Sasano H, Anderson TJ, Silverberg SG, et al. The validation of new aromatase monoclonal antibodies for immunohistochemistry – a correlation with biochemical activities in 46 cases of breast cancer. J Steroid Biochem Mol Biol 2005;95:35-9
23. Skov BG, Fischer BM, Pappot H. Oestrogen receptor beta over expression in males with non-small cell lung cancer is associated with better survival. Lung Cancer 2008;59:88-94
24. Ishibashi H, Suzuki T, Suzuki S, et al. Progesterone receptor in non-small cell lung cancer – a potent prognostic factor and possible target for endocrine therapy. Cancer Res 2005;65:6450-8
25. Suzuki T, Miki Y, Moriya T, et al. 5alpha-reductase type 1 and aromatase in breast carcinoma as regulators of in situ androgen production. Int J Cancer 2007;120:285-891
26. Jordan VC. Selective estrogen receptor modulation: concept and consequences in cancer. Cancer Cell 2004;5:207-13
27. Verma MK, Miki Y, Sasano H. Aromatase in human lung carcinoma. Steroids 2011;76:759-64
28. Speirs V, Green CA, Shaaban AM. Oestrogen receptor beta immunohistochemistry: time to get it right? J Clin Pathol 2008;61:1150-1
29. Wu CT, Chang YL, Shih JY, Lee YC. The significance of estrogen receptor beta in 301 surgically treated non-small cell lung cancers. J Thorac Cardiovasc Surg 2005;130:979-86
30. Stabile LP, Dacic S, Land SR, et al. Combined analysis of estrogen receptor beta-1 and progesterone receptor expression identifies lung cancer patients with poor outcome. Clin Cancer Res 2011;17:154-64

31. Thun MJ, Henley SJ, Burns D, et al. Lung cancer death rates in lifelong nonsmokers. J Natl Cancer Inst 2006;98:691-9

32. Mah V, Marquez D, Alavi M, et al. Expression levels of estrogen receptor beta in conjunction with aromatase predict survival in non-small cell lung cancer. Lung Cancer 2011;74:318-25

33. Paech K, Webb P, Kuiper GG, et al. Differential ligand activation of estrogen receptors ERalpha and ERbeta at AP1 sites. Science 1997;277:1508-10

34. Saville B, Wormke M, Wang F, et al. Ligand-, cell-, and estrogen receptor subtype (alpha/beta)-dependent activation at GC-rich (Sp1) promoter elements. J Biol Chem 2000;275:5379-87

35. Langer G, Bader B, Meoli L, et al. LA critical review of fundamental controversies in the field of GPR30 research. Steroids 2010;75:603-10

36. Shen H, Yuan Y, Sun J, et al. Combined tamoxifen and gefitinib in non-small cell lung cancer shows antiproliferative effects. Biomed Pharmacother 2010;64:88-92

37. Lazzara MJ, Lane K, Chan R, et al. Impaired SHP2-mediated extracellular signal-regulated kinase activation contributes to gefitinib-sensitivity of lung cancer cells with epidermal growth factor receptor-activating mutations. Cancer Res 2010;70:3843-50

Affiliation

Mohit Kumar Verma, Yasuhiro Miki, Keiko Abe, Hiromichi Niikawa & Hironobu Sasano†
†Author for correspondence
Tohoku University Graduate School of Medicine,
Department of Pathology,
2-1 Seriyo-machi, Aoba-ku,
Sendai, Miyagi-ken 980 8575, Japan
Tel: + 81 22 717 8050; Fax: + 81 22 717 8051;
E-mail: hsasano@patholo2.med.tohoku.ac.jp

IJC
International Journal of Cancer

Runt-related transcription factor 2 in human colon carcinoma: a potent prognostic factor associated with estrogen receptor

Tomohiko Sase[1,2], Takashi Suzuki[3], Koh Miura[1], Kenichi Shiiba[4], Ikuro Sato[5], Yasuhiro Nakamura[6], Kiyoshi Takagi[3], Yoshiaki Onodera[6], Yasuhiro Miki[6], Mika Watanabe[2], Kazuyuki Ishida[2], Shinobu Ohnuma[1], Hiroyuki Sasaki[1], Ryuichiro Sato[1], Hideaki Karasawa[1], Chikashi Shibata[1], Michiaki Unno[1], Iwao Sasaki[1] and Hironobu Sasano[2,6]

[1] Department of Surgery, Tohoku University Graduate School of Medicine, Sendai, Japan
[2] Department of Pathology, Tohoku University Hospital, Sendai, Japan
[3] Department of Pathology and Histotechnology, Tohoku University Graduate School of Medicine, Sendai, Japan
[4] Department of Surgery, Miyagi Cancer Center, Natori, Japan
[5] Department of Pathology, Miyagi Cancer Center, Natori, Japan
[6] Department of Pathology, Tohoku University Graduate School of Medicine, Sendai, Japan

Runt-related transcription factor 2 (RUNX2) belongs to the RUNX family of heterodimeric transcription factors, and is mainly associated with osteogenesis. Previous *in vitro* studies demonstrated that RUNX2 increased the cell proliferation of mouse and rat colon carcinoma cells but the status of RUNX2 has remained unknown in human colon carcinoma. Therefore, we examined clinical significance and biological functions of RUNX2 in colon carcinoma. RUNX2 immunoreactivity was examined in 157 colon carcinoma tissues using immunohistochemistry. RUNX2 immunoreactivity was evaluated as percentage of positive carcinoma cells [*i.e.*, labeling index (LI)]. We used SW480 and DLD-1 human colon carcinoma cells, expressing estrogen receptor-β (ER) in subsequent *in vitro* studies. RUNX2 immunoreactivity was detected in colon carcinoma cells, and the median value of RUNX2 LI was 67%. RUNX2 LI was significantly associated with Dukes' stage, liver metastasis and ERβ status. In addition, RUNX2 LI was significantly associated with adverse clinical outcome of the colon carcinoma patients, and turned out an independent prognostic factor following multivariate analysis. Results of *in vitro* studies demonstrated that both SW480 and DLD-1 cells transfected with small interfering RNA against RUNX2 significantly decreased their cell proliferation, migration and invasive properties. In addition, RUNX2 mRNA level was significantly decreased by ER antagonist in these two cells. These findings all suggest that RUNX2 is a potent prognostic factor in human colon carcinoma patients through the promotion of cell proliferation and invasion properties, and is at least partly upregulated by estrogen signals through ERβ of carcinoma cells.

Colon cancer is the third leading cause of cancer-related deaths in both men and women in the United States.[1] It is true that the recent advances in chemotherapy prolonged the survival of the patients with advanced clinical stages[2] but these results are still unsatisfactory and further studies are being required to understand the disease process and to improve the clinical outcome of the patients.

Key words: colon carcinoma, Runt-related transcription factor 2, immunohistochemistry, prognosis, estrogen receptor

Abbreviations: BSP: bone sialoprotein; ER: estrogen receptor; MMP: Matrix metalloproteinase; RUNX2: Runt-related transcription factor 2; VEGF: vascular endothelial growth factor

Additional Supporting Information may be found in the online version of this article

DOI: 10.1002/ijc.27525

History: Received 27 Jul 2011; Accepted 15 Feb 2012; Online 7 Mar 2012

Correspondence to: Hironobu Sasano, Department of Pathology, Tohoku University Graduate School of Medicine, 2-1 Seiryo-machi, Aoba-ku, Sendai, Miyagi, 980-8575, Japan, Tel.: +81 22 717 8050, Fax: +81 22 717 8051, E-mail: hsasano@patholo2.med.tohoku.ac.jp

The Runt-related transcription factor 2 (RUNX2) belongs to the RUNX family of heterodimeric transcription factors and shares a common sequence termed, the Runt domain, with other members involved in DNA binding and transactivation.[3] RUNX2 is a well-known transcription factor required in the process of bone formation or osteogenesis.[4–7] For instance, an altered chondrocyte morphology was reported in RUNX2 heterogenous mice,[8] and its deregulation was also associated with the development of osteosarcoma.[9,10]

Recently, expression of RUNX2 has been reported in several human malignancies such as prostate,[11] pancreatic,[12] thyroid[13] and breast[14] cancers, all of which highlighted the carcinogenic properties of RUNX2 in these studies. Results of previous *in vitro* studies did demonstrate that RUNX2 increased the cell proliferative activity of mouse[15] and rat[16] colon carcinoma cells, which suggests a possible role for RUNX2 also in colon carcinoma. In addition, very recently, Edvardsson *et al.*[17] conducted genome-wide expression studies in combination with gene-pathway analyses and cross-correlation to estrogen receptor-β (ERβ)-chromatin-binding sites, and demonstrated that RUNX2 expression was induced by ERβ in human colorectal carcinoma cells. However, the

status of RUNX2 has not been examined in human colon carcinoma to the best of our knowledge, and its biological and clinical significance has remained unknown. Therefore, in this study, we examined clinical significance and biological functions of RUNX2 in colon carcinoma using immunohistochemistry and *in vitro* studies.

Material and Methods

Patients and tissues

Colon carcinoma surgical pathology specimens were obtained from 157 consecutive patients (86 men and 71 women) operated at Miyagi Cancer Center (Natori, Japan) from 1994 to 2000. A mean age of these patients was 67.0 years (range 35–85 years). The mean follow-up time was 100 months (range 1–149 months), and overall survival data were available in all the patients examined. The specimens had been fixed in 10% formalin and embedded in paraffin-wax.

Review of the patients' charts revealed that neither of the patients received irradiation nor chemotherapy before the surgery. Informed consent was obtained from all the patients above and research protocol for this study was approved by the Ethics Committees at the Miyagi Cancer Center (2007–2006).

Immunohistochemistry

Mouse monoclonal antibody for human RUNX2 was purchased from Abnova Corporation (Taipei, Taiwan). The characterization of this antibody has been reported using both immunoblotting and immunohistochemistry.[18] Monoclonal antibodies for ERβ (MS-ERB13-PX1) and Ki-67 (MIB1) were purchased from GeneTex (Irvine, CA) and DAKO (Carpinteria, CA), respectively. A Histofine kit (Nichirei, Tokyo, Japan), using the streptavidin–biotin amplification method, was used in this study. The antigen–antibody complex was visualized with 3,3′-diaminobenzidine (DAB) solution [1 mM DAB, 50 mM Tris-HCl buffer (pH 7.6) and 0.006% H_2O_2], and counterstained with hematoxylin. As a negative control, normal mouse or rabbit IgG was used instead of the primary antibodies, and no immunoreactivity was detected in these tissue sections.

Immunoreactivity of RUNX2 and Ki67 was detected in the nuclei. Their immunoreactivity was evaluated in more than 1,000 carcinoma cells for each case, and subsequently, the percentage of immunoreactivity, that is, labeling index (LI), was determined. The status of ERβ immunoreactivity was evaluated using Allred score.[19] Briefly, following an evaluation of the proportion (0: none, 1: <1/100, 2: 1/100–1/10, 3: 1/10–1/3, 4: 1/3–2/3, and 5: >2/3) and immunointensity (0: none, 1: weak, 2: moderate, and 3: strong) in the carcinoma cells, the total score more than 3 was considered ERβ-positive case. An association between RUNX2 LI and clinicopathological factors of colon carcinoma patients was statistically evaluated using a correlation coefficient (r) and regression equation, Student's t test, or a one-way ANOVA and Bonferroni test. Overall survival curves were generated according to the Kaplan–Meier method and the statistical significance was calculated using the log-rank test. Both univariate and multivariate analyses were performed by a proportional hazard model (COX) using StatView 5.0 software (SAS Institute, Cary, NC), and differences with $p < 0.05$ were considered significant.

Cell lines and chemicals

Two human colon carcinoma cell lines (SW480 and DLD-1) were provided from the American Type Culture Collection (Manassas, VA). The cells were cultured in the recommended medium [L-15 Medium Leibovitz (Sigma-Aldrich, St. Louis, MO) for SW480 or RPMI1640 (Sigma-Aldrich) for DLD-1, containing 10% heat-inactivated fetal bovine serum (FBS; Sigma-Aldrich) and 1% penicillin–streptomycin (Invitrogen, Carlsbad, CA)]. A pure ER antagonist ICI 182,780[20] was purchased from Tocris Cookson (Ellisville, MO) in this study.

Real-time PCR

Total RNA was extracted from cultured cells using the RNeasy Mini Kit (Qiagen, Valencia, CA). cDNA was synthesized using a SuperScript III First-Strand Synthesis System for reverse transcription-polymerase chain reaction Kit (Invitrogen) from 5 μg of total RNA.

The LightCycler System (Roche Diagnositics GmbH, Mannheim, Germany) was used to semiquantify the mRNA expression levels by real-time PCR.[21] The primer sequences used in our study are as follows: RUNX2 (NM_004348 forward: 782–800 and reverse: 943–961),[22] ERβ (AB006590; forward: 1,460–1,480 and reverse: 1,608–1,627), and ribosomal protein L 13a (RPL13A) (NM_012423; forward: 487–509 and reverse: 588–612).[23] The mRNA level in each sample was represented as a ratio of RPL13A and was evaluated as a ratio (%) compared with that of each control.

Small interfering RNA transfection

Small interfering RNA (siRNA) oligonucleotide for RUNX2 used in this study was Stealth RNAi siRNA Duplex Oligoribonucleotides (Invitrogen), and Stealth RNAi Negative Control Duplexes (Invitrogen) was also used as the negative control. The sequence of siRNA against RUNX2 (RUNX2-HSS189448) was as follow: sense 5′-AUCUACUGUAACUU UAAUUGCUCUG-3′ and antisense 5′-CAGAGCAAUUAAA GUUACAGUAGAU-3′. siRNA against ERβ (forward 5′-GUGUGAAGCAAGAUCGCUA-3′ and reverse 5′-UAGCGA UCUUGUUUCACAC-3′) was also used in this study. siRNAs were transfected (10 nmol/L) using HiperFect transfection reagent (Qiagen GmbH, Hilden, Germany) according to the instruction manual.

Immunoblotting

The protein of SW480 and DLD1 cells was extracted using M-PER Mammalian Protein Extraction Reagent (Pierce Biotechnology, Rockford, IL) with Halt Protease Inhibitor Cocktail (Pierce Biotechnology). 20 μg of the protein (whole cell extracts) were subjected to SDS-PAGE (10% acrylamide gel).

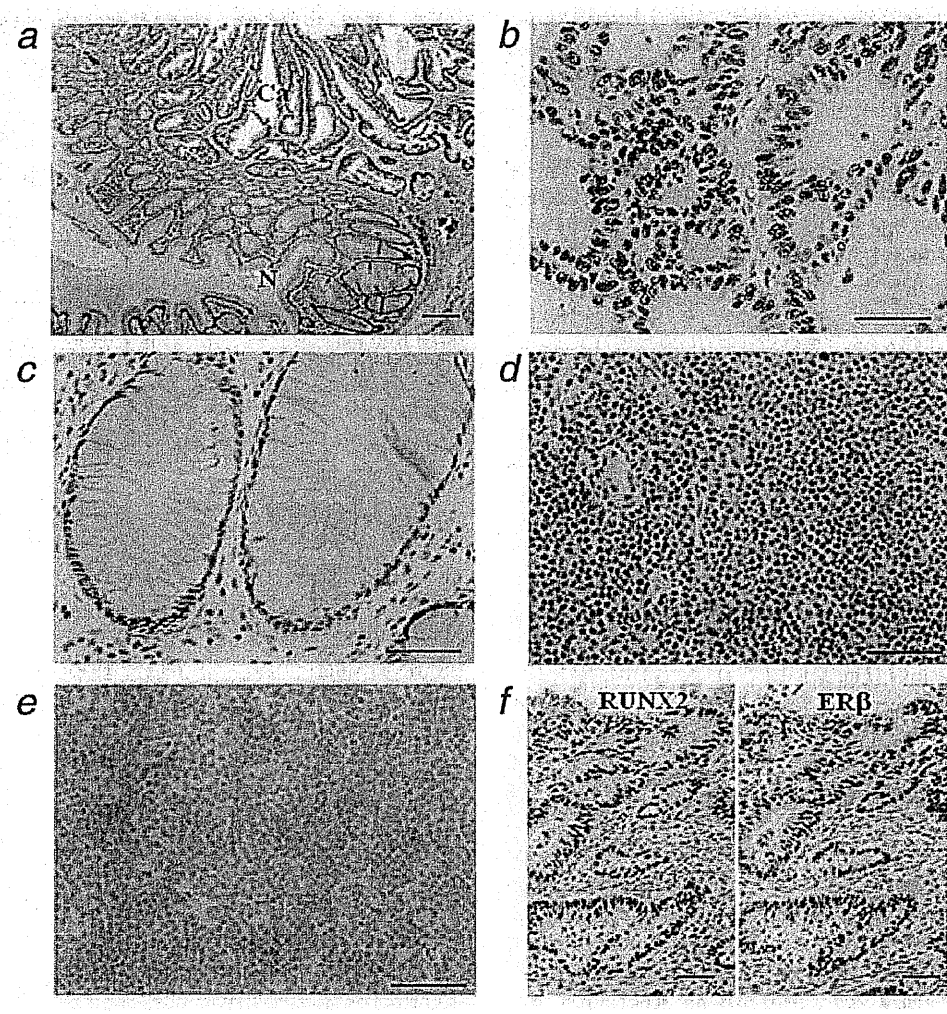

Figure 1. Representative illustrations of RUNX2 immunohistochemistry in colon carcinoma cases. (*a*) RUNX2 immunoreactivity was detected in the carcinoma cells (Ca), while almost negligible in the non-neoplastic colonic epithelium (N). Lower magnification and scale bar = 200 μm. (*c* and *d*) RUNX2 was immunolocalized in the nuclei of carcinoma cells (*b*), while focally and weakly positive in non-neoplastic colonic epithelium cells (*c*). Higher magnification and scale bar = 100 μm, respectively. (*d* and *e*) Positive (*d*) and negative (*e*) control sections of RUNX2 immunohistochemistry (same area of the lymph node). Scale bar = 100 μm, respectively. (*f*) Immunohistochemistry for RUNX2 and ERβ in the colon carcinoma on serial tissue sections (same area). Scale bar = 100 μm, respectively. [Color figure can be viewed in the online issue, which is available at wileyonlinelibrary.com.]

Following SDS-PAGE, proteins were transferred onto Hybond P polyvinylidene difluoride membrane (GE Healthcare, Buckinghamshire, UK). Primary antibodies used were anti-RUNX2 antibody used for immunohistochemistry (Abnova Corporation) and anti-β-actin antibody (AC-15, Sigma-Aldrich). Antibody–protein complexes on the blots were detected using ECL-plus Western blotting detection reagents (GE Healthcare), and the protein bands were visualized with LAS-1000 image analyzer (Fuji Photo Film, Tokyo, Japan).

Cell proliferation, migration, and invasion assays

SW480 and DLD-1 cells were transfected with RUNX2-specific siRNA or control siRNA in a six-well culture plate. In one day after transfection, these cells (approximately 1×10^4 cells/well) were transferred to 96-well culture plate and cultured in medium containing 10% FBS. Three days after the transfection, the status of cell proliferation was measured by a cell counting kit-8 (Dojindo, Kumamoto, Japan).

The migration assay was performed according to the procedure reported by Fang *et al.*[24] Briefly, 4 days after the transfection, colon carcinoma cells cultured in a six-well culture plate were carefully scratched by sterile 20-μl pipette tips, and then incubated for 24 hr. The scratched edges were imaged by phase-contrast microscopy, and the migration area was calculated using the NIH image software (http://rsb.info.nih.gov/nih-image/Default.html).[24]

Cell invasion assay was performed using a 24-well (8 μm pore size) BD Matrigel™ Invasion Chamber (BD Biosciences, Bedford, MA), according to the manufacturer's protocol. After incubation for 1 day, the noninvading cells are removed from the upper surface of the membrane using cotton swabs. The cells on the lower surface of the membrane are stained with Diff-Quik stain™ (Sysmex International Reagents, Kobe, Japan) according to the instruction manual. The total number of invading cells of the membrane was counted under the microscope.

Results

RUNX2 immunolocalization in human colon cancer

RUNX2 immunoreactivity was detected in the nuclei of the colon carcinoma cells (Figs. 1*a* and 1*b*), and the median value of RUNX2 LI was 67.0% (range 0–100%). RUNX2 immunoreactivity was weakly and focally detected in some non-neoplastic colonic epithelial cells (Fig. 1*a* and 1*c*). In the positive control, RUNX2 was mainly positive in lymphocyte of the lymph node (Fig. 1*d*), as previously reported,[25] whereas no significant immunoreactivity was detected in the negative control tissue sections (Fig. 1*e*).

Associations between RUNX2 LI and various clinicopathological parameters in colon carcinoma patients were summarized in Table 1. RUNX2 LI was significantly associated with Dukes' stage ($p = 0.04$), liver metastasis ($p = 0.02$) and ERβ status ($p = 0.02$) of the cases examined. However, no significant association was detected in other factors examined, such as patient age, gender, tumor site, depth of invasion, lymph node metastasis, peritoneal metastasis, histological differentiation and Ki67 LI. Co-localization of RUNX2 and ERβ was detected in the majority of colon carcinoma cells, when their immunohistochemistry was performed on serial tissue sections (Fig. 1*f*).

Association between RUNX2 LI and clinical outcome of the patients

As demonstrated in Figure 2*a*, higher RUNX2-LI group was significantly ($p < 0.0001$) associated with adverse clinical outcome of the patients when the 157 cases were tentatively classified into two groups according to the median value of RUNX2 LI. Similar tendencies were detected regardless of the Dukes' stage (Figs. 2*b* and 2*c*) or in the ERβ-positive cases ($n = 131$; Fig. 2*d*). Results of the univariate analysis studied by COX analysis (Table 2) demonstrated that RUNX2 LI ($p < 0.0001$), liver metastasis ($p < 0.0001$), Ki-67 LI ($p = 0.01$), lymph node metastasis ($p = 0.03$) and ERβ ($p = 0.04$) turned out significant prognostic variables for overall survival of the patients in this study. Results of the following multivariate analysis, however, showed that only RUNX2 LI ($p = 0.003$) and Ki67 LI ($p = 0.02$)[26] were independent prognostic factors. RUNX2 LI was also detected as an independent prognostic factor, when evaluated as a continuous variable in the multivariate analysis ($p = 0.0002$; data not shown).

Table 1. Association between RUNX2 LI and clinicopathological parameters in 157 colon carcinoma patients

Value	RUNX2 LI ($n = 157$)	*p*-value
Patient age[1]		0.91 ($r = -0.18$)
Gender		
Men ($n = 86$)	57.7 ± 26.6	
Women ($n = 71$)	58.7 ± 27.2	0.46
Tumor site[2]		
Proximal ($n = 94$)	58.2 ± 26.4	
Distal ($n = 63$)	57.8 ± 24.7	0.91
Dukes' stage		
A+B ($n = 83$)	52.5 ± 23.1	
C+D ($n = 74$)	64.3 ± 19.4	**0.04**
Depth of invasion		
Submucosa-muscularis propria ($n = 27$)	47.0 ± 28,6	
Through muscularis propria ($n = 130$)	60.4 ± 27.5	0.14
Lymph node metastasis		
Positive ($n = 66$)	63.9 ± 19.8	
Negative ($n = 91$)	53.8 ± 28.4	0.15
Liver metastasis		
Positive ($n = 20$)	70.9 ± 13.7	
Negative ($n = 137$)	56.0 ± 26.4	**0.02**
Peritoneal metastasis		
Positive ($n = 4$)	69.0 ± 10.8	
Negative ($n = 153$)	57.6 ± 25.8	0.38
Histological differentiation[3]		
Well ($n = 44$)	60.4 ± 25.5	
Moderate + poor ($n = 103$)	58.0 ± 25.2	0.61
ERβ status		
Positive ($n = 131$)	60.1 ± 25.1	
Negative ($n = 26$)	47.0 ± 25.9	**0.02**
Ki67 LI[1,4]		0.17 ($r = 0.26$)

[1]The association was statistically evaluated using a correlation coefficient (r) and regression equation. The data were presented as mean ± SD. *p*-values of less than 0.05 were considered significant, and are shown in bold. [2]Proximal colon included in ascending and transverse colon. [3]Cases of mucinous adenocarcinoma were excluded in this study. [4]The mean Ki67 LI of these patients was 49.8% (range 2–96%).

Effects of RUNX2 on cell proliferation, migration and invasion in colon carcinoma cells

In this study, we transfected two human colon carcinoma cells (SW480 and DLD-1) with specific siRNA against RUNX2 to examine biological functions of RUNX2 in these cells. RUNX2 mRNA level compared to RPL13A examined by real-time PCR analysis was 1.8% in SW480 cells and 1.1% in DLD-1 cells (data not shown), and RUNX2 LI evaluated

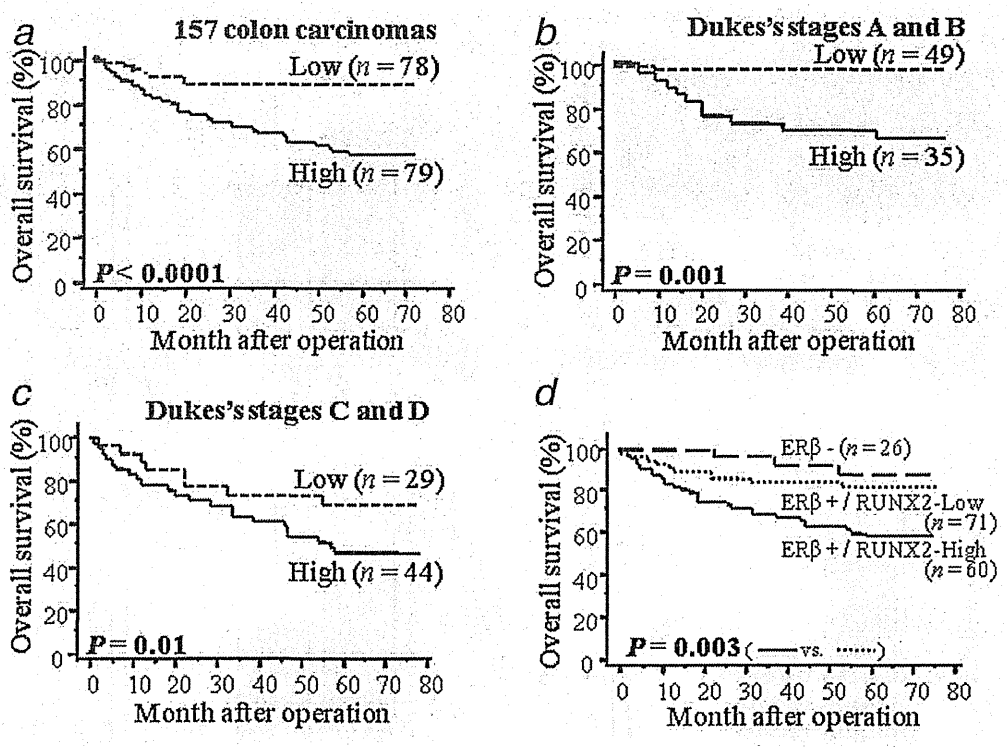

Figure 2. Overall survival curves of 157 colon carcinoma patients according to the RUNX2 immunoreactivity by Kaplan–Meier method. (*a*) RUNX2 immunoreactivity was significantly associated with worse prognosis (p <0.0001 by the log-rank test), when RUNX2 LI was further classified into two groups according to the median value. (*b* and *c*) Similar tendency was also detected in the patient groups of Dukes' stages *a* and *b* (*b*: $n = 84$) and the groups of Dukes' stages *c* and *d* (C: $n = 73$). (*d*) An association between ERβ status and clinical outcome of the patients according to the status of RUNX2 immunoreactivity. ERβ-positive cases were further categorized into two subgroups according to the median value of RUNX2 LI. Significant association ($p = 0.003$) was detected between ERβ+/RUNX2-High and ERβ+/RUNX2-Low groups.

Table 2. Univariate and multivariate analysis of overall survival of 157 colon carcinoma patients

	Univariate		Multivariate
Variable	*p*	*p*	Hazard ratio (95% CI)
RUNX2 LI (high/low)[1]	<0.0001[2]	0.003	1.0 (1.0–1.1)
Liver metastasis (+/−)	<0.0001[2]	0.05	
Ki67 LI (high/low)[1]	0.01[2]	0.02	1.0 (0.9–1.0)
Lymph node metastasis (+/−)	0.03[2]	0.62	
ERβ (+/−)	0.04[2]	0.20	
Gender (women/men)	0.13		
Histological differentiation[3] (moderate + poor/well)	0.51		

[1]The cases were categorized into two groups according to the median value.[26] [2]Data were considered significant in univariate analysis, and were examined in multivariate analysis. [3]Cases of mucinous adenocarcinoma were excluded in this study ($n = 147$). Statistically significant values ($p < 0.05$) were in boldface.

in the cell block in these cell lines was 67.4 and 81.8%, respectively (Fig. 3*a*, upper panel). RUNX2 mRNA expression level was markedly decreased in these cells transfected with specific siRNA against RUNX2 both at 2 and 4 days after the transfection compared to those transfected with control siRNA, and the ratio of RUNX2 mRNA level compared to that in the control siRNA at 2 and 4 days was 14.1 and 3.6% in SW480 and 7.8 and 5.9% in DLD-1 cells, respectively. Immunoblotting analysis subsequently confirmed decreased RUNX2 protein expression in SW480 and DLD1 cells transfected with RUNX2 siRNA for 3 days (Fig. 3*a*, lower panel).

As demonstrated in Figure 3*b*, cell proliferative activity was significantly lower both in SW480 and DLD-1 cells transfected with siRNA against RUNX2 ($p < 0.01$ and 0.74-fold in SW480, and $p < 0.01$ and 0.83-fold in DLD-1) than those transfected with control siRNA at 3 days after the transfection. In the migration assay, the migration area was significantly decreased in these cells transfected with siRNA against RUNX2 at 1 day after scratch (SW480: $p < 0.001$ and 0.43-fold, and DLD-1: $p < 0.001$ and 0.63-fold; Figure 3*c* and Supporting Information Fig. S1). In addition, the number of invading cells was significantly lower in the cells transfected with RUNX2 siRNA than those transfected with control siRNA at 3 days after the transfection (SW480: $p < 0.05$ and 0.69-fold, and DLD-1: $p < 0.01$ and 0.66-fold; Fig. 3*d*).

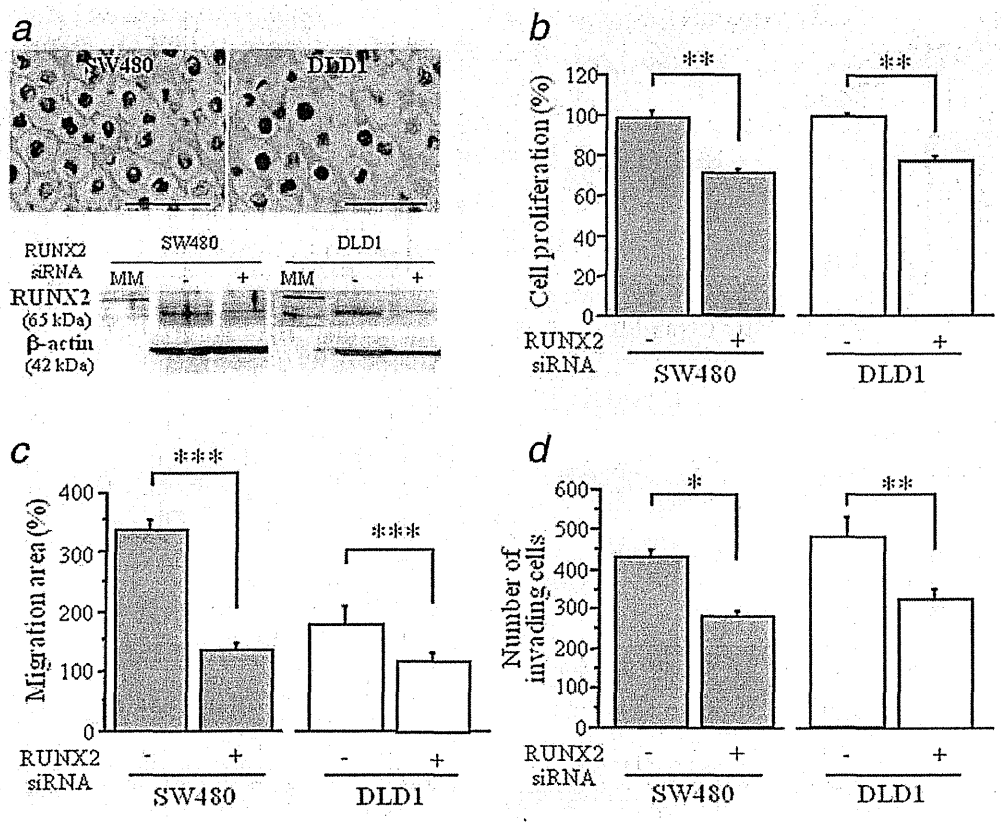

Figure 3. Effects of RUNX2 expression on cell proliferation, migration and invasive properties in colon carcinoma cells. (*a*) Expression of RUNX2 protein in SW480 and DLD1 cells. Upper panel demonstrated results of immunocytochemistry of RUNX2 in SW480 (left upper panel) and DLD-1 (right upper panel) cells. Cell blocks from formalin-fixed and paraffin-embedded specimens, and bar = 50 μm, respectively. Lower panel demonstrated immunoblotting of RUNX2 in SW480 (left lower panel) and DLD1 (right lower panel) cells transfected with specific RUNX2 siRNA (*i.e.*, RUNX2 siRNA: +) or control siRNA (*i.e.*, RUNX2 siRNA: –). The protein of cells was extracted at 3 days after the transfection. MM: molecular marker. (*b–d*): Results of proliferation (*b*), migration (*c*) and invasion (*d*) assays in SW480 (gray bar) and DLD-1 (open bar) cells were summarized. These cells were transfected with specific RUNX2 siRNA or control siRNA. Data were presented as mean ± SD ($n = 3$), respectively. *; $p < 0.05$, **; $p < 0.01$ and ***; $p < 0.001$. The statistical analyses were performed using Student's *t* test. [Color figure can be viewed in the online issue, which is available at wileyonlinelibrary.com.]

Regulation of RUNX2 expression by ERβ in colon carcinoma cells

As described earlier, RUNX2 immunoreactivity was positively associated with ERβ status in colon carcinomas examined (Table 1 and Fig. 1*f*), which suggests a possible interaction of RUNX2 and ERβ in colon carcinoma cells. Therefore, to further investigate this interaction, we treated the cells positive for ERβ but negative for ERα with a pure ER antagonist ICI 182,780.[27,28] As summarized in Figures 4*a* and 4*b*, ICI 182,780 significantly inhibited the RUNX2 mRNA level of these cells in a dose-dependent manner, significant at 5 μM of ICI 182,780 treatment compared to the basal level (SW480: $p < 0.05$ and 0.26-fold, DLD-1: $p < 0.05$ and 0.21-fold). RUNX2 mRNA level was also significantly ($p < 0.05$, respectively) suppressed in SW480 (0.66-fold) and DLD1 (0.68-fold) cells transfected with ERβ siRNA (Fig. 4*c*). Conversely, ERβ mRNA level itself was not significantly different (SW480: $p = 0.18$ and 0.89-fold, and DLD-1: $p = 0.96$ and 0.98-fold) between the cells treated with RUNX2 and control siRNA (Fig. 4*d*).

When SW480 and DLD1 cells were treated with 5 μM of ICI 182,780 for 3 days, their cell proliferation and invasive properties were both significantly suppressed compared to the control or nontreated cells [cell proliferation activity: $p < 0.01$ in SW480 and $p < 0.05$ in DLD1 (Supporting Information Fig. S2A), and invasive property: $p = 0.12$ in SW480 and $p < 0.05$ in DLD1 (Supporting Information Fig. S2B)].

Discussion

In this study, we first demonstrated that RUNX2 immunoreactivity was frequently detected in colon carcinoma cells but negligible in non-neoplastic colonic mucosa and turned out

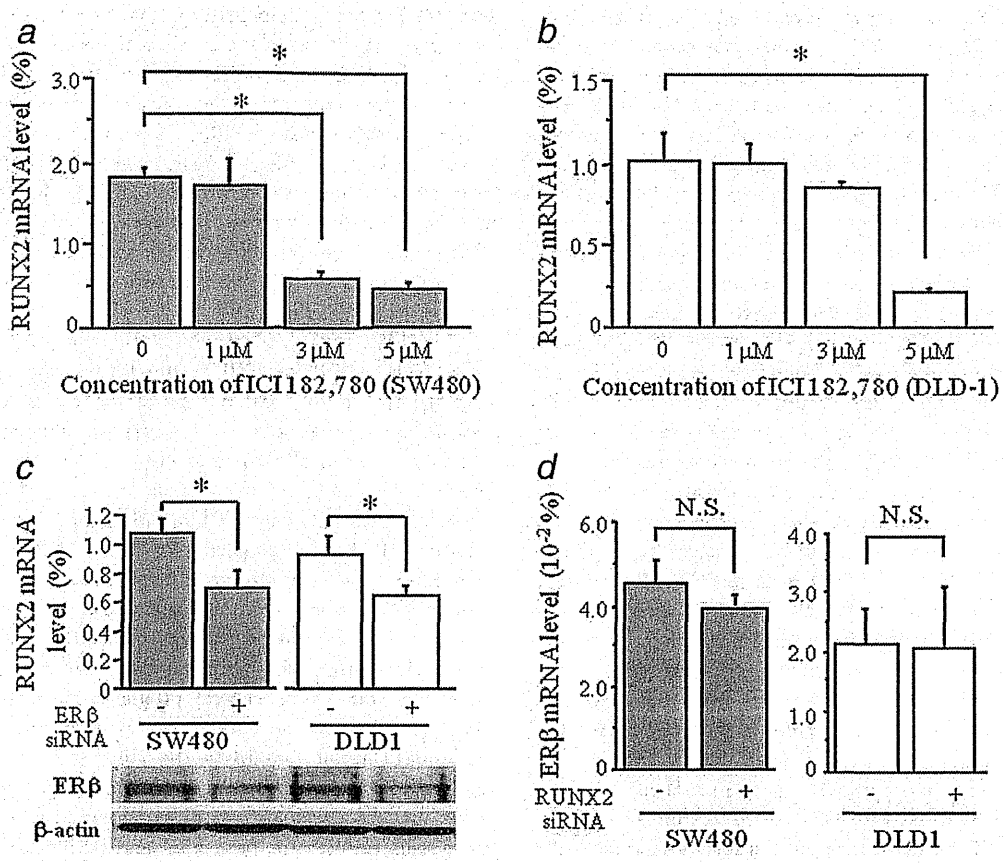

Figure 4. Regulation of RUNX2 expression in colon carcinoma cells. (*a* and *d*) Effects of ICI 182,780 on RUNX2 mRNA expression in SW480 (*a*) and DLD-1 (*b*) cells by real-time PCR analysis. The cells were treated with indicated concentrations of ICI 182,780 for 3 days. (*c*) Effects of ERβ siRNA on RUNX2 mRNA expression in SW480 (gray bar) and DLD-1 (open bar) cells. These cells were transfected with specific ERβ siRNA (ERβ siRNA: +) or control siRNA (ERβ siRNA: −), and RUNX2 mRNA level was examined using real-time PCR analysis. Data were presented as mean ± SD ($n = 3$), respectively. *; $p < 0.05$, and the statistical analyses were performed using Student's *t* test. Lower panel summarized ERβ protein level in each specimens according to the results of immunoblot analysis. (*d*) Effects of RUNX2 on ERβ mRNA expression in SW480 (gray bar) and DLD-1 (open bar) cells. ERβ mRNA level was evaluated by real-time PCR analysis in the cells treated with specific RUNX2 siRNA (RUNX2 siRNA: +) or control siRNA (RUNX2 siRNA: −). Data were presented mean ± SD ($n = 3$), respectively. *; $p < 0.05$, and N.S.; not significant. The statistical analyses were performed using one-way ANOVA and Bonferroni test (*a* and *b*) or Student's *t* test (*c* and *d*).

as an independent adverse prognostic factor of the patients. RUNX2 immunolocalization was previously reported in prostate,[11] pancreatic,[12] thyroid[13] and breast[14] carcinoma tissues. RUNX2 expression was also reported to be elevated in carcinoma cells compared to normal epithelium in both pancreatic and breast carcinoma, and was significantly associated with adverse clinical outcome in breast carcinoma patients.[12,14] Results of our present study in colon carcinoma are in general consistent with results of these reports above and suggest that RUNX2 immunoreactivity in carcinoma cells serves as a potent marker of aggressive clinical behavior in colon carcinoma patients.

In our present study, RUNX2 immunoreactivity was positively associated with Dukes' stage and liver metastasis in colon carcinoma patients. Results of the subsequent *in vitro* experiments also indicated that RUNX2 significantly promoted cell proliferation, migration and invasive properties of colon carcinoma cells. The processes of carcinoma metastasis generally consist of multisteps including migration, invasion, dissemination into the blood vessel and proliferation at the site of metastatic organ and the metastasis is the greatest cause of death in colon carcinoma patients. Results of previously reported *in vitro* studies demonstrated that RUNX2 expression induced the cell proliferation of mouse[15] and rat[16] colon carcinoma cell lines. RUNX2 stimulated transcription of osteopontin, which was also reported to increase metastatic properties in human colon carcinoma cells[29] and CT26 mouse colorectal carcinoma cells.[15] However, it is also true

that RUNX2 expression was recently reported to be modulated by TGF-β1 in CC531 rat colorectal carcinoma cells,[16] which subsequently induced angiogenesis and metastasis of colon carcinoma.[30] RUNX2 expression was also reported to be closely associated with the expression of vascular endothelial growth factor,[31] matrix metalloproteinase[32,33] and bone sialoprotein.[34] Therefore, it is suggested that RUNX2 plays important roles in the growth and metastasis of colon carcinoma cells through its wide spectrums of biological functions. However, it is also true that RUNX2 immunoreactivity was not significantly associated with depth of invasion, lymph node metastasis, peritoneal metastasis or Ki67 LI in the colon carcinoma cases examined in this study, which was not necessarily consistent with the results of our *in vitro* studies. Further examinations are required to clarify the precise molecular functions of RUNX2 in colon carcinoma cells.

Results of our present study demonstrated that the status of RUNX2 immunoreactivity was positively associated with that of ERβ in colon carcinoma cells, suggesting a possible interaction of RUNX2 and ERβ in these cells. ER consists of ERα and ERβ in humans, and ERβ is predominantly expressed in some malignancies including colon,[35] while the great majority of breast carcinoma cells expresses ERα.[36] Das *et al.*[37] reported that ERα and ERβ expression was decreased in MCF-7 breast carcinoma cells transfected with RUNX2, but Matsumoto *et al.*[38] demonstrated that estradiol enhanced bone morphologic protein-induced RUNX2 expression in ERα and ERβ positive C2C12 mouse myoblast cells. Results of our present *in vitro* studies also showed that RUNX2 mRNA expression was decreased by ICI 182,780 both in SW480 and DLD-1 colon carcinoma cells in a dose-dependent manner but the level of ERβ mRNA expression was not significantly changed in these cells transfected with RUNX2 siRNA. SW480 and DLD-1 cells used in our present study have been known negative for ERα but positive for ERβ,[27,28] and ICI 182,780 is a well-characterized pure antagonist of ERs.[39,40] Very recently, Edvardsson *et al.*[17] reported that ERβ induced RUNX2 expression through its direct binding to the promoter in colorectal carcinoma cells, which is consistent with results of our present study. Therefore, these findings above all suggest that RUNX2 expression is at least reasonably postulated to be partly upregulated by estrogenic signals through ERβ in colon carcinoma cells.

Results of previous studies regarding estrogen actions in colon carcinoma cells are in general inconsistent in terms of its biological actions and its significance has still remained unclear. Results of various epidemiological studies have generally suggested a protective effect of hormone replacement therapy on the risk of developing colorectal carcinomas, which also implied that estrogen exerts a protective effect against colorectal cancer in relatively early stage of carcinoma development.[41] However, Janakiram *et al.*[42] reported that ERβ acted as a colon tumor promoter and raloxifene, a selective ER modulator, protected colon carcinogenesis. In addition, we previously demonstrated that intratumoral estrogen levels were significantly higher than those in non-neoplastic colonic mucosa, and were significantly associated with adverse clinical outcome of the colon carcinoma patients.[43]

Clinical significance of ERβ has been proposed in the colon carcinomas, but has not been necessarily determined. An association between loss of ERβ and adverse clinicopathological factors has been reported by several investigators,[44–46] but Wong *et al.*[35] reported that higher expression of ERβ was positively associated with the presence of lymph node metastasis in the patients. Little is known on an association between ERβ status and prognosis of colon carcinoma, and Fang *et al.*[47] reported ERβ as the better prognostic factor, whereas, Sato *et al.*[43] did not detect any significant correlation. In our present study, ERβ status was significantly associated with worse clinical outcome of 157 colon carcinoma patients, and results of our present *in vitro* studies demonstrated that ER antagonist ICI 182,780 suppressed cell proliferation and invasive properties of both SW480 and DLD1 cells. ER is in general known to activate the transcription of various target genes and estrogenic functions are usually determined by expression patterns or profiles of these target genes. Considering the fact that high RNUN2 group was associated with worse clinical prognosis than low RUNX2 group in ERβ-positive cases in our present study (Fig. 2*d*), inconsistent results regarding the correlation between ERβ status and clinical outcome of colon carcinoma patients above may be partly due to different ratios of colon carcinoma cells positive for both ERβ and RUNX2 examined in their cohorts.

In summary, RUNX2 immunoreactivity was frequently detected in colon carcinoma tissues, and the median value of RUNX2 LI was 67% in our present study. The RUNX2 LI was positively associated with Dukes' stage, liver metastasis and ERβ status of the patients and turned out as an independent prognostic factor of these patients. Results of our *in vitro* studies also demonstrated that both SW480 and DLD-1 human colon carcinoma cells transfected with specific siRNA against RUNX2 significantly decreased the cell proliferation, migration and invasive properties of carcinoma cells. In addition, RUNX2 mRNA expression was significantly inhibited by a pure ER antagonist ICI 182,780 in these cells positive for ERβ. These *in vivo* and *in vitro* findings suggest that RUNX2 is a potent prognostic factor in human colon carcinoma patients through the promotion of cell proliferation, migration and invasive properties of carcinoma cells and its expression may at least be partly induced by estrogen signals through ERβ.

Acknowledgements

The authors appreciate the skillful technical assistance of Mr. Katsuhiko Ono (Department of Pathology, Tohoku University Graduate School of Medicine, Sendai, Japan), Dr. Akihiro Yamamura, Dr. Kyouhei Ariake, Ms. Emiko Shibuya, Ms. Keiko Inabe, and Ms. Hiroko Fujimura (Department of Surgery, Tohoku University Graduate School of Medicine, Sendai, Japan, respectively).

References

1. American Cancer Society. Cancer facts & figures 2007. Atlanta: American Cancer Society, 2007.
2. Colucci G, Gebbia V, Paoletti G, Giuliani F, Caruso M, Gebbia N, Cartenì G, Agostara B, Pezzella G, Manzione L, Borsellino N, Misino A, et al. Phase III randomized trial of FOLFIRI versus FOLFOX4 in the treatment of advanced colorectal cancer: a multicenter study of the Gruppo Oncologico Dell'Italia Meridionale. *J Clin Oncol* 2005;23:4866–75.
3. Ito Y. Oncogenic potential of the RUNX gene family: 'Overview'. *Oncogene* 2004;23: 4198–208.
4. Ducy P, Zhang R, Geoffroy V, Ridall AL, Karsenty G. Osf2/Cbfa1: a transcriptional activator of osteoblast differentiation. *Cell* 1997;89:747–54.
5. Komori T, Yagi H, Nomura S, Yamaguchi A, Sasaki K, Deguchi K, Shimizu Y, Bronson RT, Gao YH, Inada M, Sato M, Okamoto R et al. Targeted disruption of Cbfa1 results in a complete lack of bone formation owing to maturational arrest of osteoblasts. *Cell* 1997;89:755–64.
6. Otto F, Thornell AP, Crompton T, Denzel A, Gilmour KC, Rosewell IR, Stamp GW, Beddington RS, Mundlos S, Olsen BR, Selby PB, Owen MJ. Cbfa1, a candidate gene for cleidocranial dysplasia syndrome, is essential for osteoblast differentiation and bone development. *Cell* 1997;89: 765–71.
7. Mundlos S, Otto F, Mundlos C, Mulliken JB, Aylsworth AS, Albright S, Lindhout D, Cole WG, Henn W, Knoll JH, Owen MJ, Mertelsmann R, et al. Mutations involving the transcription factor CBFA1 cause cleidocranial dysplasia. *Cell* 1997;89:773–9.
8. Zheng Q, Zhou G, Morello R, Chen Y, Garcia-Rojas X, Lee B. Type X collagen gene regulation by Runx2 contributes directly to its hypertrophic chondrocyte-specific expression in vivo. *J Cell Biol* 2003; 162:833–42.
9. San Martin IA, Varela N, Gaete M, Villegas K, Osorio M, Tapia JC, Antonelli M, Mancilla EE, Pereira BP, Nathan SS, Lian JB, Stein JL, et al. Impaired cell cycle regulation of the osteoblast-related heterodimeric transcription factor Runx2-Cbfbeta in osteosarcoma cells. *J Cell Physiol* 2009;221:560–71.
10. Pereira BP, Zhou Y, Gupta A, Leong DT, Aung KZ, Ling L, Pho RW, Galindo M, Salto-Tellez M, Stein GS, Cool SM, van Wijnen AJ, et al. Runx2, p53, and pRB status as diagnostic parameters for deregulation of osteoblast growth and differentiation in a new pre-chemotherapeutic osteosarcoma cell line (OS1). *J Cell Physiol* 2009;221:778–88.
11. Brubaker KD, Vessella RL, Brown LG, Corey E. Prostate cancer expression of runt-domain transcription factor Runx2, a key regulator of osteoblast differentiation and function. *Prostate* 2003;56:13–22.
12. Kayed H, Jiang X, Keleg S, Jesnowski R, Giese T, Berger MR, Esposito I, Löhr M, Friess H, Kleeff J. Regulation and functional role of the Runt-related transcription factor-2 in pancreatic cancer. *Br J Cancer* 2007;97:1106–15.
13. Endo T, Ohta K, Kobayashi T. Expression and function of Cbfa-1/Runx2 in thyroid papillary carcinoma cells. *J Clin Endocrinol Metab* 2008;93:2409–12.
14. Onodera Y, Miki Y, Suzuki T, Takagi K, Akahira J, Sakyu T, Watanabe M, Inoue S, Ishida T, Ohuchi N, Sasano H. Runx2 in human breast carcinoma: its potential roles in cancer progression. *Cancer Sci* 2010;101: 2670–5.
15. Wai PY, Mi Z, Gao C, Guo H, Marroquin C, Kuo PC. Ets-1 and runx2 regulate transcription of a metastatic gene, osteopontin, in murine colorectal cancer cells. *J Biol Chem* 2006;281:18973–82.
16. Georges R, Adwan H, Zhivkova M, Eyol E, Bergmann F, Berger MR. Regulation of osteopontin and related proteins in rat CC531 colorectal cancer cells. *Int J Oncol* 2010;37:249–56.
17. Edvardsson K, Ström A, Jonsson P, Gustafsson JÅ, Williams C. Estrogen receptor β induces antiinflammatory and antitumorigenic networks in colon cancer cells. *Mol Endocrinol* 2011;25:969–79.
18. Mak IW, Cowan RW, Popovic S, Colterjohn N, Singh G, Ghert M. Upregulation of MMP-13 via Runx2 in the stromal cell of Giant Cell Tumor of bone. *Bone* 2009;45:377–86.
19. Allred DC, Clark GM, Elledge R, Fuqua SA, Brown RW, Chamness GC, Osborne CK, McGuire WL. Association of p53 protein expression with tumor cell proliferation rate and clinical outcome in node-negative breast cancer. *J Natl Cancer Inst* 1993;85:200–6.
20. Howell A, Osborne CK, Morris C, Wakeling AE. ICI 182,780 (Faslodex): development of a novel, "pure" antiestrogen. *Cancer* 2000;89:817–25.
21. Dumoulin FL, Nischalke HD, Leifeld L, von dem Bussche A, Rockstroh JK, Sauerbruch T, Spengler U. Semi-quantification of human C-C chemokine mRNAs with reverse transcription/real-time PCR using multi-specific standards. *J Immunol Methods* 2000;241:9–19.
22. Miki Y, Suzuki T, Hatori M, Igarashi K, Aisaki KI, Kanno J, Nakamura Y, Uzuki M, Sawai T, Sasano H. Effects of aromatase inhibitors on human osteoblast and osteoblast-like cells: a possible androgenic bone protective effects induced by exemestane. *Bone* 2007;40:876–87.
23. Suzuki T, Inoue A, Miki Y, Moriya T, Akahira J, Ishida T, Hirakawa H, Yamaguchi Y, Hayashi S, Sasano H. Early growth responsive gene 3 in human breast carcinoma: a regulator of estrogen-meditated invasion and a potent prognostic factor. *Endocr Relat Cancer* 2007;14: 279–92.
24. Fang YJ, Pan ZZ, Li LR, Lu ZH, Zhang LY, Wan DS. MMP7 expression regulated by endocrine therapy in ERbeta-positive colon cancer cells. *J Exp Clin Cancer Res* 2009;28: 132–9.
25. Ehrhardt GR, Hijikata A, Kitamura H, Ohara O, Wang JY, Cooper MD. Discriminating gene expression profiles of memory B cell subpopulations. *J Exp Med* 2008;205:1807–17.
26. Fluge Ø, Gravdal K, Carlsen E, Vonen B, Kjellevold K, Refsum S, Lilleng R, Eide TJ, Halvorsen TB, Tveit KM, Otte AP, Akslen LA, et al. Expression of EZH2 and Ki-67 in colorectal cancer and associations with treatment response and prognosis. *Br J Cancer* 2009;101:1282–9.
27. Arai N, Strom A, Rafter JJ, Gustafsson JA. Estrogen receptor beta mRNA in colon cancer cells: growth effects of estrogen and genistein. *Biochem Biophys Res Commun* 2000;270:425–31.
28. Lauber SN, Ali S, Gooderham NJ. The cooked food derived carcinogen 2-amino-1-methyl-6-phenylimidazo[4,5-b] pyridine is a potent oestrogen: a mechanistic basis for its tissue-specific carcinogenicity. *Carcinogenesis* 2004;12:2509–17.
29. Likui W, Hong W, Shuwen Z. Clinical significance of the upregulated osteopontin mRNA expression in human colorectal cancer. *J Gastrointest Surg* 2010; 14:74–81.
30. Bellone G, Carbone A, Tibaudi D, Mauri F, Ferrero I, Smirne C, Suman F, Rivetti C, Migliaretti G, Camandona M, Palestro G, Emanuelli G, et al. Differential expression of transforming growth factors-beta1, -beta2 and -beta3 in human colon carcinoma. *Eur J Cancer* 2001;37:224–33.
31. Zelzer E, Glotzer DJ, Hartmann C, Thomas D, Fukai N, Soker S, Olsen BR. Tissue specific regulation of VEGF expression during bone development requires Cbfa1/Runx2. *Mech Dev* 2001;106:97–106.
32. Pratap J, Javed A, Languino LR, van Wijnen AJ, Stein JL, Stein GS, Lian JB. The Runx2 osteogenic transcription factor regulates matrix metalloproteinase 9 in bone metastatic cancer cells and controls cell invasion. *Mol Cell Biol* 2005;25: 8581–91.

33. Selvamurugan N, Kwok S, Partridge NC. Smad3 interacts with JunB and Cbfa1/Runx2 for transforming growth factor-beta1-stimulated collagenase-3 expression in human breast cancer cells. *J Biol Chem* 2004;279:27764–73.
34. Barnes GL, Javed A, Waller SM, Kamal MH, Hebert KE, Hassan MQ, Bellahcene A, Van Wijnen AJ, Young MF, Lian JB, Stein GS, Gerstenfeld LC. Gerstenfeld LC. Osteoblast-related transcription factors Runx2 (Cbfa1/AML3) and MSX2 mediate the expression of bone sialoprotein in human metastatic breast cancer cells. *Cancer Res* 2003;63:2631–7.
35. Wong NA, Malcomson RD, Jodrell DI, Groome NP, Harrison DJ, Saunders PT. ERβ isoform expression in colorectal carcinoma: an in vivo and in vitro study of clinicopathological and molecular correlates. *J Pathol* 2005;207:53–60.
36. Ali S, Coombes RC. Estrogen receptor alpha in human breast cancer: occurrence and significance. *J Mammary Gland Biol Neoplasia* 2000;5:271–81.
37. Das K, Leong DT, Gupta A, Shen L, Putti T, Stein GS, van Wijnen AJ, Salto-Tellez M. Positive association between nuclear Runx2 and oestrogen-progesterone receptor gene expression characterises a biological subtype of breast cancer. *Eur J Cancer* 2009;45; 2239–48.
38. Matsumoto Y, Otsuka F, Takano M, Mukai T, Yamanaka R, Takeda M, Miyoshi T, Inagaki K, Sada KE, Makino H. Estrogen and glucocorticoid regulate osteoblast differentiation through the interaction of bone morphogenetic protein-2 and tumor necrosis factor-alpha in C2C12 cells. *Mol Cell Endocrinol* 2010;325; 118–127.
39. Howell A, Robertson JF, Quaresma Albano J, Aschermannova A, Mauriac L, Kleeberg UR, Vergote I, Erikstein B, Webster A, Morris C. Fulvestrant, formerly ICI 182,780, is as effective as anastrozole in postmenopausal women with advanced breast cancer progressing after prior endocrine treatment. *J Clin Oncol* 2002;20: 3396–403.
40. Niikawa H, Suzuki T, Miki Y, Suzuki S, Nagasaki S, Akahira J, Honma S, Evans DB, Hayashi S, Kondo T, Sasano H. Intratumoral estrogens and estrogen receptors in human non-small cell lung carcinoma. *Clin Cancer Res* 2008;14: 4417–26.
41. Chen MJ, Longnecker MP, Morgenstern H, Lee ER, Frankl HD, Haile RW. Recent use of hormone replacement therapy and the prevalence of colorectal adenomas. *Cancer Epidemiol Biomarkers Prev* 1998;7: 227–30.
42. Janakiram NB, Steele VE, Rao CV. Estrogen receptor-beta as a potential target for colon cancer prevention: chemoprevention of azoxymethane-induced colon carcinogenesis by raloxifene in F344 rats. *Cancer Prev Res* 2009;2:52–9.
43. Sato R, Suzuki T, Katayose Y, Miura K, Shiiba K, Tateno H, Miki Y, Akahira J, Kamogawa Y, Nagasaki S, Yamamoto K, Ii T, et al. Steroid sulfatase and estrogen sulfotransferase in colon carcinoma: regulators of intratumoral estrogen concentrations and potent prognostic factors. *Cancer Res* 2009;69:914–22.
44. Konstantinopoulos PA, Kominea A, Vandoros G, Sykiotis GP, Andricopoulos P, Varakis I, Sotiropoulou-Bonikou G, Papavassiliou AG. Oestrogen receptor beta (ERbeta) is abundantly expressed in normal colonic mucosa, but declines in colon adenocarcinoma paralleling the tumour's dedifferentiation. *Eur J Cancer* 2003;39:1251–8.
45. Jassam N, Bell SM, Speirs V, Quirke P. Loss of expression of oestrogen receptor beta in colon cancer and its association with Dukes' staging. *Oncol Rep* 2005;14: 17–21.
46. Castiglione F, Taddei A, Degl'Innocenti DR, Buccoliero AM, Bechi P, Garbini F, Chiara FG, Moncini D, Cavallina G, Marascio L, Freschi G, Gian LT. Expression of estrogen receptor beta in colon cancer progression. *Diagn Mol Pathol* 2008;17:231–36.
47. Fang YJ, Lu ZH, Wang F, Wu XJ, Li LR, Zhang LY, Pan ZZ, Wan DS. Prognostic impact of ERβ and MMP7 expression on overall survival in colon cancer. *Tumour Biol* 2010;31:651–8.

Journal of Pathology
J Pathol (2012)
Published online in Wiley Online Library
(wileyonlinelibrary.com) DOI: 10.1002/path.4019

ORIGINAL PAPER

Aromatase inhibitor treatment of breast cancer cells increases the expression of *let-7f*, a microRNA targeting *CYP19A1*

Yukiko Shibahara,[1] Yasuhiro Miki,[1] Yoshiaki Onodera,[1] Shuko Hata,[1] Monica SM Chan,[1,2–4] Christopher CP Yiu,[1,3] Tjing Y Loo,[1,2–4] Yasuhiro Nakamura,[1] Jun-ichi Akahira,[1] Takanori Ishida,[5] Keiko Abe,[1] Hisashi Hirakawa,[6] Louis WC Chow,[2–4,7] Takashi Suzuki,[1] Noriaki Ouchi[5] and Hironobu Sasano[1]*

[1] *Department of Pathology, Tohoku University Graduate School of Medicine, 2-1 Seiryo-machi, Aoba-ku, Sendai, Miyagi 980-8575, Japan*
[2] *UNIMED Medical Institute, Comprehensive Centre for Breast Diseases, 10/F, Luk Kwok Centre, 72 Gloucester Road, Wanchai, Hong Kong*
[3] *Department of Surgery, Li Ka Shing Faculty of Medicine, The University of Hong Kong, Queen Mary Hospital, 102 Pokfulam Road, Hong Kong*
[4] *Clinical Trial Centre, Li Ka Shing Faculty of Medicine, The University of Hong Kong, Queen Mary Hospital, 102 Pokfulam Road, Hong Kong*
[5] *Department of Surgery, Tohoku University Graduate School of Medicine, 2-1 Seiryo-machi, Aoba-ku, Sendai, Miyagi 980-8575, Japan*
[6] *Department of Surgery, Tohoku Kosai Hospital, 2-3-11 Kokubun-cho, Aoba-ku, Sendai, Miyagi 980-0803, Japan*
[7] *Organisation of Oncology and Translational Research, Unit A, 9/F, CNT Commercial Building, 302 Queen's Road Central, Hong Kong*

**Correspondence to: Hironobu Sasano, Department of Pathology, Tohoku University Graduate School of Medicine, 2-1 Seiryo-machi, Aoba-ku, Sendai, Miyagi 980-8575, Japan. e-mail: hsasano@patholo2.med.tohoku.ac.jp*

Abstract

Aromatase inhibitors (AIs) are considered the gold standard of endocrine therapy for oestrogen receptor-positive postmenopausal breast cancer patients. AI treatment was reported to result in marked alterations of genetic profiles in cancer tissues but its detailed molecular mechanisms have not been elucidated. Therefore, we profiled miRNA expression before and after treatment with letrozole in MCF-7 co-cultured with primary breast cancer stromal cells. Letrozole significantly altered the expression profiles of cancer miRNAs *in vitro*. Among the elevated miRNAs following letrozole treatment, computational analysis identified *let-7f*, a tumour-suppressor miRNA which targeted the *aromatase* gene (*CYP19A1*) expression. Quantitative real-time PCR assay using MCF-7 and SK-BR-3 cells as well as clinical specimens of a neoadjuvant study demonstrated a significant inverse correlation between *aromatase* mRNA and *let-7f* expression. In addition, high *let-7f* expression was significantly correlated with low aromatase protein levels evaluated by both immunohistochemistry and the western blotting method in breast cancer cases. Results of 3'UTR luciferase assay also demonstrated the actual *let-7f* binding sites in *CYP19A1*, indicating that *let-7f* directly targets the *aromatase* gene. Subsequent WST-8 and migration assays performed in *let-7f*-transfected MCF-7 and SK-BR-3 cells revealed a significant decrement of their proliferation and migration. These findings all demonstrated that *let-7f*, a tumour suppressor miRNA in breast cancer, directly targeted the *aromatase* gene and was restored by AI treatment. Therefore, AIs may exert tumour-suppressing effects upon breast cancer cells by suppressing *aromatase* gene expression via restoration of *let-7f*.

Keywords: aromatase inhibitors; *CYP19A1*; *let-7*; breast cancer

Received 24 October 2011; Revised 7 February 2012; Accepted 21 February 2012

Conflict of interest statement: HS received educational research grants from Novartis Japan Oncology and Pfizer Japan Oncology. YM received educational research grants from Pfizer Japan. The other authors disclosed no potential conflicts of interest.

Introduction

The treatment for oestrogen receptor-positive (ER+) postmenopausal breast cancer patients has advanced significantly in the past decades. Tamoxifen was considered the gold standard for endocrine therapy but the third-generation aromatase inhibitors (AIs) confer clinical benefits over tamoxifen in terms of decreased recurrence rates and increased relapse-free survival [1–4]. AIs are generally considered to work on ER+ breast cancer cells by depleting oestrogens through inhibiting the conversion of androgens to oestrogens, eliminating the pivotal sources of oestrogen necessary for tumour growth. Third-generation AIs include the non-steroidal inhibitor anastrozole and letrozole and the steroidal inhibitor exemestane. Both types of AIs have been extensively used in clinical practice but their detailed mechanisms have not been clarified.

Alterations in the protein-coding regions of genes following AI treatment have been reported, including genes associated with oestrogen regulation (*KIAA0101, ZWINT, IRS1*, and *TFF1*) and cell cycle progression (*CDK1, CCNB1*, and *CKS2*) in breast cancer cells [5]. In addition, Mackay *et al* reported that *aromatase* (*CYP19A1*) mRNA itself was significantly down-regulated by AIs [6]. microRNAs (miRNAs) are short non-protein coding RNAs known to play key regulatory roles in various cellular processes. Dysregulation

of miRNAs has been recently reported to play a key role in various therapeutic responses [7]. The equilibrium of miRNA expression is frequently disturbed in human cancers, with the miRNAs themselves acting as tumour suppressors or oncogenes [8]. miRNA profiling has led to the discovery of miRNAs that are aberrantly expressed in breast cancer including tumour suppressor miRNAs (*miR-206, miR-125, miR-17-5p, let-7, miR-34a*, and *miR-31*) and oncogenic miRNAs (*miR-21, miR-155, miR-10b*, and *miR-373/520c*) [9]. Widespread alterations of miRNA profiles by oestrogen administration have also been reported recently [10], which suggest a profound connection between oestrogen and tumour growth at the miRNA level.

We therefore performed miRNA PCR array using a third-generation AI, letrozole-treated breast cancer cell line to demonstrate the potential involvement of miRNAs in AI treatment. The results of this *in vitro* study revealed that letrozole treatment significantly altered the global expression profiles of miRNAs. Among tumour-suppressor miRNAs increased by letrozole treatment, computational analysis identified *let-7f* and its putative roles for directly targeting *CYP19A1* [11]. We further evaluated the correlation between aromatase expression and the status of *let-7f* in breast cancer cases and demonstrated an inverse correlation between *let-7f* and *aromatase* mRNA/protein expression. These results provide new insights into the roles of miRNAs in AI treatment of ER+ breast cancer patients.

Materials and methods

Chemicals

Letrozole was obtained from Novartis Pharma AG (Basel, Switzerland).

Cell lines and culture conditions

The human breast cancer cell lines MCF-7 and SK-BR-3 were provided by the Cell Resource Center for Biomedical Research, Tohoku University (Sendai, Japan). MCF-7 and SK-BR-3 cells were cultured in RPMI 1640 (Sigma-Aldrich, St Louis, MO, USA) and supplemented with 10% fetal bovine serum (FBS; Nichirei, Tokyo, Japan). Primary stromal cells employed in this study were provisionally designated 32N, isolated from operated breast cancer specimens using collagenase treatment [12], and maintained in RPMI 1640 with 10% FBS. MCF-7 and 32N were each cultured in RPMI 1640 with dextran-coated charcoal (DCC)–FBS for 3 days before each experiment to exhaust endogenous oestrogen.

Co-culture system and AI treatment

The co-culture method was employed in this study to induce *aromatase* mRNA expression in MCF-7 cells according to our previous reports [13]. This co-culture method was previously reported to induce aromatase through an interaction between stromal and breast cancer cells and has been considered useful for evaluating the effects of medications on breast cancer patients, mimicking their *in vivo* intratumoural microenvironment [13]. Transwell cultures were established in six-well plates or 100-mm dishes using ThinCert™ (0.4 μm pore; Greiner Bio-One, Germany) in order to promote physical separation of the stromal and carcinoma cell lines. MCF-7 cells were cultured in transwell chambers in the absence or presence of 32N cells and were cultivated on the bottom of the plates or dishes (MCF-7co). After 48 h of cultivation using this co-culture system, letrozole (10^{-8} mol/l) was applied for 48 h (MCF-7co/le). MCF-7 and 32N cells were separated and total RNA was isolated from three samples each for MCF-7, MCF-7co, and MCF-7co/le using the TRIzol method according to the manufacturer's instructions. SK-BR-3 cells were not co-cultured with stromal cells because SK-BR-3 was known to express relatively strong aromatase activity, according to a previous report [13].

Patients and tissue collection

Three frozen breast cancer tissue specimens from ER+, postmenopausal patients receiving neoadjuvant AI treatment (3 months of letrozole, 2.5 mg daily) were obtained from the Celecoxib Anti-Aromatase Neoadjuvant Trial (CAAN Trial) [14], a clinical trial conducted at The University of Hong Kong and Queen Mary Hospital, Hong Kong. Eleven frozen ER+ breast cancer tissue samples used for real-time PCR and nine frozen breast cancer tissue samples used for western blotting, which did not receive any prior treatment, were obtained from Tohoku University Hospital, Sendai, Japan. Informed consent was obtained from all patients. The research protocol for this study was approved by the Ethics Committee at The University of Hong Kong (HK1821-02) and Tohoku University School of Medicine (2010-509). Prior to RNA extraction, the frozen sections were stained with haematoxylin and eosin for detailed histological evaluation under light microscopy. Briefly, the entire frozen tissues were disrupted using a tissue homogenizer and total RNA including miRNA was extracted using TRIzol Reagent (Invitrogen, Carlsbad, CA, USA).

Laser capture microdissection (LCM) in 10% formalin-fixed, paraffin-embedded (FFPE) tissues

Twenty FFPE breast cancer tissues retrieved from the surgical pathology files of Tohoku Kosai Hospital were sectioned at a thickness of 8 μm. Carcinoma components were subsequently laser-transferred with care under light microscopic evaluation. LCM was performed using mmi CellCut (Molecular Machines & Industries AG, Glattbrug, Switzerland). MiRNA was extracted using a PureLink miRNA Isolation Kit (Invitrogen). cDNA was also synthesized using an RT^2 miRNA First Strand kit (Qiagen, Hilden, Germany). Research protocols for this study were approved by the

Ethics Committee at both Tohohu Kosai Hospital (No H17.8.5) and Tohoku University School of Medicine (2009-203), respectively.

Transfection

Hsa-let-7f (Genolution Pharmaceuticals, Seoul, Korea) was transfected into MCF-7 cells by Lipofectamine 2000 (Invitrogen) with 5 or 10 nM mature microRNA molecules for 24, 48, and 72 h. Scramble siRNA (Genolution Pharmaceuticals) was used as a negative control.

Quantitative reverse transcription real-time PCR of *aromatase* mRNA

For real-time PCR on the expression of *aromatase* mRNA in MCF-7, SK-BR-3, and clinical samples, total RNA was extracted as described above. cDNA was synthesized using a QuantiTect reverse transcription kit (Qiagen). Real-time PCR was carried out using the LightCycler System and FastStart DNA Master SYBR Green I (Roche Diagnostics, Mannheim, Germany). The PCR primer sequences used in this study were as follows: *aromatase* (X13 589), forward 691–reverse 806; and the *ribosomal protein L13a* (*RPL13A*) (NM_012 423), forward 487–reverse 612 [13]. cDNA of known *aromatase* concentration and the housekeeping gene *RPL13A* were used to generate standard curves for real-time quantitative PCR in order to determine the quantity of target cDNA transcript. The mRNA level in each case was represented as a ratio of *RLP13A*.

Quantitative reverse transcription real-time PCR of miRNA

For cancer-related miRNA profiling in MCF-7 cells, total RNA was extracted as described above. MCF-7co and MCF-7co/le were analysed for the expression of a panel of 88 cancer-related miRNAs using RT^2 miRNA PCR Array Human Cancer MAH-102A (Qiagen). For *let-7f* quantification in MCF-7 and SK-BR-3 cells, frozen breast cancer tissues and FFPE specimens, total RNA or miRNA was extracted as described above and quantified using RT^2 miRNA qPCR assay (Qiagen). *U6* was used for normalization; conditions employing no templates and/or reverse transcription were included as negative controls. PCR was performed on an ABI7500 Real-Time PCR System (Applied Systems, Foster City, CA, USA). Data analysis was performed with the web-based software package for the miRNA PCR array system (http://www.sabiosciences.com/pcr/arrayanalysis.php).

Target prediction of miRNA

TargetScan 5.1 (http://www.targetscan.org/), MiRanda (http://www.microrna.org/), PicTar (http://pictar.mdc-berlin.de/), and PITA (http://genie.weizmann.ac.il/pubs/mir07/mir07_notes.html) were used to search for putative targets of miRNAs that were altered by letrozole treatment and also for miRNAs which target *aromatase*.

Immunohistochemistry

The antibodies used in this study were as follows: ERα (ER1D5; Immunotech SA, Marseilles, France); progesterone receptor (MAB429; Chemicon International Inc, Temecula, CA, USA); Ki-67 (MIB1; DakoCytomation Co Ltd, Kyoto, Japan); and aromatase [13]. For aromatase, the approximate percentage of cells staining (proportion score) was classified into the following four groups: 0, < 1%; 1, 1–25%; 2, 26–50%; and 3, >50% immuno-positive cells. The relative immuno-intensity of aromatase positive cells was classified as follows: 0, no immunoreactivity; 1, weak; 2, moderate; and 3, intense immunoreactivity. Aromatase immunoreactivity was evaluated as a total score composed of the proportion score plus the relative immuno-intensity score [13].

Western blotting

Nine frozen breast cancer tissue samples were available for western blotting. Tissue protein was extracted using M-PER Mammalian Protein Extraction Reagent (Pierce Biotechnology, Rockford, IL, USA) with Halt Protease Inhibitor Cocktail (Pierce Biotechnology). Following SDS-PAGE (10% acrylamide gel), proteins were transferred onto Hybond P polyvinylidene difluoride membrane (GE Healthcare, Buckinghamshire, UK). The primary antibodies used in this study were aromatase [13] and β-actin (AC-15; Sigma-Aldrich). Antibody–protein complexes on the blots were detected using ECL Plus western blotting detection reagents (GE Healthcare). The protein bands were visualized and the immuno-intensity of specific bands was quantified using an LAS-1000 image analyzer (Fuji Photo Film Co, Tokyo, Japan). The relative immuno-intensity of aromatase was evaluated as a ratio of β - actin in each sample examined in our study.

Luciferase reporter assay

A pmirGLO Dual-Luciferase miR Target Expression Vector was used for 3'UTR luciferase assays (Promega Corporation, Madison, WI, USA). The following primer sequences were used: *CYP19A1* forward primers, F1 (5′-AAAGCTAGCCTAGAGAAGGCTGG TCAGTAC-3′) and F2 (5′-AAAGCTAGCTAAAGAA CGTGGTCAGAGTAG-3′); *CYP19A1* reverse primers, R1 (5'AAACTCGAGGTTAAATCTCTCAGGTAACT G-3′) and R2 (5′-AAACTCGAGCTCTGACCACGT TCTTTACTG-3′) (Figures 4a and 4b). The annealed oligonucleotides were ligated into the XhoI/NheI site of pmirGLO Dual-Luciferase miR Target Expression Vector. The constructs were then verified by sequencing. MCF-7 cells were co-transfected with 5 nM scramble siRNA or *hsa-let-7f* (Genolution Pharmaceuticals) and 5 ng of pmirGLO Dual-Luciferase miRNA Target

Expression Vectors using Lipofectamine 2000 (Invitrogen). Vectors containing the target sequence were amplified using F2 and R1 (92 base pairs) and F1 and R2 (1164 base pairs) (named pGL-V1 and pGL-V2, respectively); vectors not containing the target sequence were amplified using F1 and R2 (1100 base pairs) (named pGL-V3). The DNA sequences of these three constructs were confirmed by DNA sequencing. Luciferase assay was performed using the Dual-Luciferase Reporter Assay System (Promega) at 24 h following the transfection according to the manufacturer's protocols. Firefly luciferase activity was normalized to Renilla luciferase activity.

Cell proliferation assay

MCF-7 and SK-BR-3 cells were each cultured in low-adhesion 24-well plates (AGC Techno Glass Co, Ltd, Chiba, Japan) and transfected with *let-7f* (5, 10, and 50 nM). Cell proliferation was measured using the WST-8 colorimetric assay (Cell Counting Kit-8; Dojindo Laboratories, Kumamoto, Japan [15]). Briefly, WST-8 reagent solution was added to each well, after which the microplates were incubated for 2 h at 37 °C. The absorbance at 450 nm was then measured using a cell counter (Sysmex CDA-500, Sysmex Corporation, Hyogo, Japan).

Wound healing assay

Cell migration was analysed using a modified wound healing assay. Briefly, the wound healing assay was performed using ibidi Culture-Insert (ibidi GmbH, Munich, Germany) inserted in 24-well plates. After the cells became confluent, a cell-free gap of 500 μm was created by removing the Culture-Insert. Cells migrating into the gap region were observed by microscopy and we took photographs of the cell-free gap areas of three different fields using an Olympus digital camera.

Statistical analysis

All statistical analyses were performed using StatView (USA). A p value of less than 0.05 was regarded as statistically significant.

Results

Effects of letrozole treatment on *aromatase* mRNA expression in breast cancer cell lines

Co-culture of MCF-7 with stromal cells significantly increased *aromatase* mRNA levels, which is consistent with the results of our previously reported study [13]. Forty-eight hours of letrozole treatment resulted in a significant decrease of *aromatase* mRNA in MCF-7 (control MCF-7co = 0.00082 ± 0.0001646; MCF-7co/le: 6 h = 0.000671 ± 0.0000222, 12 h = 0.000837 ± 0.0001793, 24 h = 0.00077 ± 0.0000557 ± ?, 48 h = 0.00034 ± 0.00005*, *$p < 0.05$) (Figure 1a). Forty-eight hours of letrozole treatment in SK-BR-3 also resulted in a 23.9% decrease of *aromatase* mRNA (data not shown).

Alterations of microRNA profiles following letrozole treatment in breast cancer cell lines

Results of the PCR array in letrozole-treated MCF-7 cells demonstrated that five miRNAs were down-regulated and 13 miRNAs were up-regulated by more than two-fold (Figure 1b). These miRNAs were further analysed for possible targeting of the *aromatase* gene (*CYP19A1*) using the multiple prediction programs described above. From this analysis, *let-7f* was calculated to contain the optimum sequence for directly targeting *CYP19A1*. Therefore, we subsequently focused on *let-7f*. Significant up-regulation of *let-7f* by 48 h of letrozole treatment in MCF-7 cells as well as SK-BR-3 cells was confirmed by the RT^2 miRNA qPCR assay ($p < 0.05$, Figure 1c). We also performed qRT-PCR in paired breast cancer cases receiving neoadjuvant letrozole treatment in order to verify these findings in clinical cases. Two out of three cases demonstrated marked up-regulation of *let-7f* (Figure 2).

Relationship between *let-7f* and aromatase expression levels in breast cancer tissues

The results of multiple target prediction algorithms revealed that *let-7f* negatively regulated *aromatase* gene expression. We then examined the possible correlation between *aromatase* mRNA and *let-7f* expression from 11 frozen breast cancer tissues. Elevated *aromatase* mRNA expression was significantly associated with low *let-7f* expression in these cases (Figure 3a, $p < 0.05$).

For examination of the correlation between *let-7f* and aromatase protein, immunohistochemistry and western blotting were utilized. The amount of *let-7f* expression in breast cancer cells isolated by laser capture microdissection was compared with that of immunohistochemical aromatase reactivity in 20 cases. Higher *let-7f* expression was significantly associated with a lower total score of aromatase immunoreactivity (Figures 3b and 3c, $p < 0.05$). The results of western blotting also indicated that *let-7f* expression and aromatase protein levels were inversely correlated (Figure 3d, $Y = 0.965 - 0.386 \times X$, $R^2 = 0.275$, $p = 0.0255$). These findings all demonstrate an inverse correlation between the expression of *let-7f* and aromatase in breast cancer.

Correlation between *let-7f* and *CYP19A1* in breast cancer cells

Transient transfection of pGL-V1 and pGL-V2 (target sequence included) in the presence of *let-7f* resulted in a significant decrease of luciferase activity compared with that of scramble siRNA but transfection of pGL-V3 (target sequence not included) did not result in a significant loss of luciferase activity (Figure 4). These results confirmed the role of *let-7f* in regulating

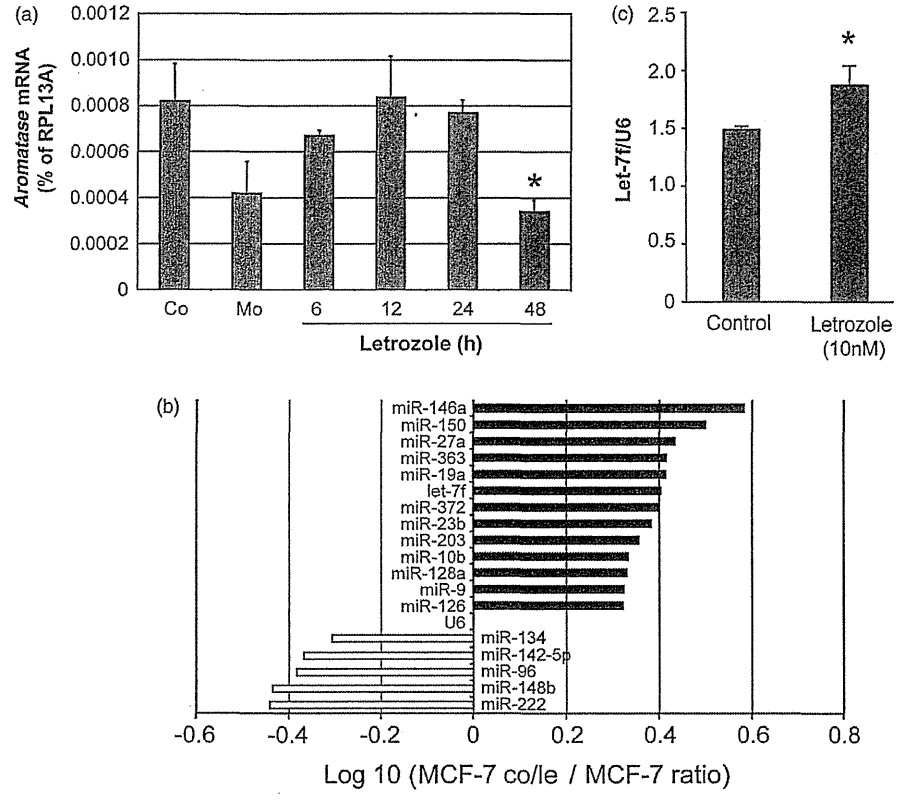

Figure 1. (a) *Aromatase* mRNA expression of MCF-7 was up-regulated by co-culture with primary stromal cells obtained from human breast cancer tissues and down-regulated by subsequent letrozole treatment. Values for *aromatase* mRNA are depicted as per cent expression to *RPL13A* by quantitative RT-PCR. MCF-7 cells were co-cultured with stromal cells for 48 h. Stromal cells were then removed and MCF-7 cells received 6, 12, 24 or 48 h of AI treatment. $^*p < 0.05$ versus MCF-7co. This experiment was independently performed in triplicate. (b) MiRNAs which were up-regulated or down-regulated by letrozole treatment relative to MCF-7/co by more than two-fold were included. Values of miRNAs were normalized to *U6*. The miRNAs were ranked according to the fold changes. This experiment was performed twice independently. (c) *Let-7f* expression was up-regulated by 48 h of letrozole treatment in SK-BR-3 cells. Values for *let-7f* were normalized to *U6*. This experiment was independently performed in triplicate.

CYP19A1 expression by actual binding to the target sequence within the 3'UTR of *CYP19A1*.

The effects of *let-7f* miRNA on *in vitro* proliferation and migration of MCF-7 and SK-BR-3 cells

The level of *let-7f* expression was significantly increased following *let-7f* transfection (data not shown). At 24 h post-transfection, the densities of the MCF-7 cells transfected with 50 nM *let-7f* were significantly lower than those of the cells transfected with scramble siRNA (control miRNA = 0.615 ± 0.057, *let-7f* = 0.2313 ± 0.027, $^*p < 0.05$, relative levels). At 48 and 72 h, the results of the WST-8 assays demonstrated significantly lower cell numbers in MCF-7 cells treated with 5, 10, and 50 nM *let-7f* compared with scramble siRNA-transfected MCF-7 cells [48 h: control miRNA = 1.109 ± 0.096, *let-7f* (5 nM) = 0.722 ± 0.055*, *let-7f* (10 nM) = 0.286 ± 0.019*, *let-7f* (50 nM) = 0.118 ± 0.008*; 72 h: control miRNA = 1.680 ± 0.126, *let-7f* (5 nM) = 0.599 ± 0.166*, *let-7f* (10 nM) = 0.136 ± 0.016, *let-7f* (50 nM) = 0.099 ± 0.011*; $^*p < 0.05$, relative levels] (Figures 5a–5c). The densities of SK-BR-3 cells transfected with 10 nM *let-7f* were also significantly decreased compared with those of the control group at 48 h (Figure 5d) [control miRNA = 0.563 ± 0.026, *let-7f* (5 nM) = 0.501 ± 0.011, *let-7f* (10 nM) = 0.463 ± 0.027*; $^*p < 0.05$].

In the wound healing assay, at 48–72 h following the gap creation, *let-7f* transfection resulted in a significant decrease of cellular migration into the gap regions in MCF-7 cells, which widened the cell-free gap by 18.5%* and 29.6%* at 10 nM, 48 and 72 h, respectively, compared with miR-control transfected cells ($^*p < 0.05$) (Figures 6a–6c). SK-BR-3 cells were slower growing compared with MCF-7 cells but *let-7f* transfection for 96 h significantly inhibited cell migration and widened the cell-free gap by 13.6%* and 11.4%* at 5 and 10 nM, respectively, compared with the control group ($^*p < 0.05$) (Figure 6d).

Discussion

We have shown that AI treatment can increase the expression of tumour-suppressing miRNAs. This interaction is important as miRNAs constitute a novel gene target network by regulating the expression of several hundred target genes, including important oncogenes